



**AFRL-RW-EG-TR-2014-005**

## **Particulate Meso-scale Mechanics Diagnostics: Magnetic Sensors for Dynamic State Orientation**

---

**David Lambert  
William Cooper**

**Air Force Research Laboratory  
Munitions Directorate  
Ordnance Division (RWM)  
Eglin AFB, FL 32542-5910**

**Ibrahim Tansel**

**Mechanical and Mechanical Engineering Dept.  
Florida International University  
Miami, FL 33174**

**Keith Jamison  
Science Applications International Corporation  
Marietta, GA 30068**

**December 2013**

**Final Report**

**Distribution A: Approved for public release; distribution unlimited.  
Approval Confirmation 96 ABW/PA # 96ABW-2013-0401, dated  
December 2013.**

**AIR FORCE RESEARCH LABORATORY, MUNITIONS DIRECTORATE**

**Air Force Materiel Command ■ United States Air Force ■ Eglin Air Force Base**

## NOTICE AND SIGNATURE PAGE

### Report contains Limited Government Purpose Rights Information


Using Government drawings, specifications, or other data included in this document for any purpose other than Government procurement does not in any way obligate the U.S. Government. The fact that the Government formulated or supplied the drawings, specifications, or other data does not license the holder or any other person or corporation; or convey any rights or permission to manufacture, use, or sell any patented invention that may relate to them.

The Government's rights to use, modify, reproduce, release, perform, display, or disclose technical data contained in this report are restricted by paragraph (b)(2) of the Rights in Technical Data – Noncommercial Items clause (DFARS 252.227-7013 (Nov 1995)) contained in the above identified contract. No restrictions apply after the expiration date shown above. Any reproduction of technical data or portions thereof marked with this legend must also reproduce the markings.

Qualified requestors may obtain copies of this report from the Defense Technical Information Center (DTIC) <<http://www.dtic.mil/dtic/index.html>>.

AFRL-RW-EG-TR-2014-005 HAS BEEN REVIEWED AND IS APPROVED FOR PUBLICATION IN ACCORDANCE WITH ASSIGNED DISTRIBUTION STATEMENT.

FOR THE DIRECTOR:

  
Digitally signed by  
LAMBERT.DAVID.E.1043478644  
DN: c=US, o=U.S. Government,  
ou=DoD, ou=PKI, ou=USAF,  
cn=LAMBERT.DAVID.E.1043478644  
Date: 2014.01.27 15:50:48 -06'00'

---

DAVID E. LAMBERT  
Lead, Core Technical Competency  
Ordnance Division

MATYAC.M  
ATTHEW.J.1  
230244568  
Digitally signed by  
MATYAC.MATTHEW.J.123024456  
8  
DN: c=US, o=U.S. Government,  
ou=DoD, ou=PKI, ou=USAF,  
cn=MATYAC.MATTHEW.J.123024  
4568  
Date: 2014.02.10 15:11:26 -06'00'

---

MATTHEW MATYAC  
Technical Advisor  
Damage Mechanisms Branch

This report is published in the interest of scientific and technical information exchange, and its publication does not constitute the Government's approval or disapproval of its ideas or findings.

This page is intentionally left blank

REPORT DOCUMENTATION PAGE				Form Approved OMB No. 0704-0188	
Public reporting burden for this collection of information is estimated to average 1 hour per response, including the time for reviewing instructions, searching existing data sources, gathering and maintaining the data needed, and completing and reviewing this collection of information. Send comments regarding this burden estimate or any other aspect of this collection of information, including suggestions for reducing this burden to Department of Defense, Washington Headquarters Services, Directorate for Information Operations and Reports (0704-0188), 1215 Jefferson Davis Highway, Suite 1204, Arlington, VA 22202-4302. Respondents should be aware that notwithstanding any other provision of law, no person shall be subject to any penalty for failing to comply with a collection of information if it does not display a currently valid OMB control number. <b>PLEASE DO NOT RETURN YOUR FORM TO THE ABOVE ADDRESS.</b>					
1. REPORT DATE (DD-MM-YYYY) 30-01-2014		2. REPORT TYPE Final		3. DATES COVERED (From - To) 1 Nov 2012 – 31 Oct 2013	
4. TITLE AND SUBTITLE  Particulate Meso-scale Mechanics Diagnostics: Magnetic Sensors for Dynamic State Orientation				5a. CONTRACT NUMBER	
				5b. GRANT NUMBER	
				5c. PROGRAM ELEMENT NUMBER 6.1PE	
6. AUTHOR(S) David Lambert (1), William Cooper (1), Ibrahim Tansel (2), Keith Jamison (3)				5d. PROJECT NUMBER 3002	
				5e. TASK NUMBER DW	
				5f. WORK UNIT NUMBER 25	
7. PERFORMING ORGANIZATION NAME(S) AND ADDRESS(ES) (1) Air Force Research Laboratory, Munitions Directorate 101 W. Eglin Blvd, Eglin AFB FL 32542-5910 (2) Mechanical and Materials Engineering Dept., Florida International Univ. 10555 West Flagler St., Miami, FL 33174 (3) Science Applications International Corp. 4901 Olde Towne Parkway, Suite 200, Marietta, GA 30068				8. PERFORMING ORGANIZATION REPORT NUMBER  AFRL-RW-EG-TR-2014-005	
9. SPONSORING / MONITORING AGENCY NAME(S) AND ADDRESS(ES)  Air Force Office of Scientific Research Arlington, VA 22203 Program Officer: Dr. Jennifer Jordan				10. SPONSOR/MONITOR'S ACRONYM(S)	
				11. SPONSOR/MONITOR'S REPORT NUMBER(S)	
12. DISTRIBUTION / AVAILABILITY STATEMENT  Distribution A: Approved for public release; distribution unlimited. Approval Confirmation 96 ABW/PA # 96ABW-2013-0401, dated Dec 2013.					
13. SUPPLEMENTARY NOTES DISTRIBUTION STATEMENT INDICATING AUTHORIZED ACCESS IS ON THE COVER PAGE AND BLOCK 12 OF THIS FORM. DATA RIGHTS RESTRICTIONS AND AVAILABILITY OF THIS REPORT ARE SHOWN ON THE NOTICE AND SIGNATURE PAGE.					
14. ABSTRACT This program was successful in producing a state-of-the art capability, resulting in the development and implementation of the following: A unique horizontal/vertical precision-ballistics gun system, multiple wave mechanics diagnostics, and two experimental configurations were developed and employed in this research. The diagnostics developed and implemented include a redundant induction-coil system, B-dot (rate change of magnetic field) sensor coils and analysis system for dynamic 5DOF state measurement, a network of flush-mounted surface pressure gages (initial size of $\phi$ 6.35 mm, final size $\phi$ 1.26 mm), fiber optic break wires, colored particulate mechanics layering method, chemical fixing/sectioning of target, and Scanning Electron Microscope (SEM) particle analysis techniques. This document captures details of the last year (of a three year effort) with an Executive Summary covering the early years and tying the efforts together.					
15. SUBJECT TERMS Particulate Mechanics, B-dot sensor, optimization					
16. SECURITY CLASSIFICATION OF:			17. LIMITATION OF ABSTRACT  SAR	18. NUMBER OF PAGES  XXX	19a. NAME OF RESPONSIBLE PERSON David E. Lambert
a. REPORT UNCLASSIFIED	b. ABSTRACT UNCLASSIFIED	c. THIS PAGE UNCLASSIFIED			19b. TELEPHONE NUMBER (include area code) 850-882-7991

This page is intentionally left blank

## PREFACE

This report was prepared at the Damage Mechanisms Branch of the Air Force Research Laboratory, Ordnance Division, Munitions Directorate (AFRL/RWMW), Eglin Air Force Base, Florida. The efforts detailed in this report were funded by the Air Force Office of Scientific Research (AFOSR). The significant amount of work was performed by Prof. Ibrahim Tansel of Florida International University while on summer research sabbatical under the Summer Faculty Fellowship Program (SFFP).

This page is intentionally left blank

## Table of Contents

List of Figures .....	x
1.0 SUMMARY .....	1
2.0 INTRODUCTION .....	1
3.0 BACKGROUND .....	1
4.0 MAGNETIC SENSOR METHOD .....	4
5.0 PROCEDURE OF REMOTE MAGNETIC SENSOR.....	4
5.1 Theoretical Background .....	5
5.1.1 Modeling the voltage generation at an induction coil with the motion of a dipole: .....	5
5.1.2 Modeling the trajectory of a projectile:.....	6
5.1.3 Calculation of the orientation of the projectile: .....	7
5.1.4 The Nelder-Mead simplex algorithm: .....	8
5.2 Experimental Set-up.....	8
5.3 Simulation Study .....	9
5.4 Proposed Procedure for Monitoring the Motion of a Magnetic Projectile .....	11
6.0 RESULTS AND DISCUSSIONS.....	14
6.1 Performance of two tracking approaches which estimated 6 and 12 parameters .....	14
6.2 Effect of number and location of the magnetic sensors on the estimations.....	17
6.3 Evaluation of the performances of different optimization algorithms and selection of the best procedure for estimation of the parameters.....	21
6.3.1 Performance of the best approach (fminsearch + nlinfit) on simulated data: .....	22
6.3.2 Performance of the best approach (fminsearch + nlinfit) on experimental data:.....	29
7.0 CONCLUSION .....	31
8.0 FUTURE WORK .....	32
9.0 ACKNOWLEDGEMENTS .....	33

## List of Figures

Figure 1. The Dipole and Induction Field at the Origin .....	6
Figure 2. Configuration of Six Magnetic Sensors for Monitoring the Motion of the Projectile.....	9
Figure 3. Configuration of Eight Magnetic Sensors for Monitoring the Motion of the Projectile .....	9
Figure 4. Configuration of Ten Magnetic Sensors for Monitoring the Motion of the Projectile .....	10
Figure 5. Configuration of Twelve Magnetic Sensors for Monitoring the Motion of the Projectile.....	10
Figure 6. The Procedure used to Generate the Simulation Data .....	11
Figure 7. Proposed Procedure for Estimation of the Trajectory and Orientation of the Projectile .....	12
Figure 8. Proposed Procedure for Estimation of the Position and Orientation.....	13
Figure 9. Proposed Procedure for Estimation of the Position, Field Strength and their Rates to Avoid B-field Estimations.....	13
Figure 10. The Position Estimation with Tracking Approach after B-field Estimation.....	14
Figure 11. Theoretical and Estimated Vector Components of Dipole Strength .....	15
Figure 12. Pitch and Yaw Orientation Estimation with Tracking Approach after B-field Estimation (positive is to the right).....	15
Figure 13. Position Estimation with Tracking Approach which use the Voltage Readings of Two Consecutive Samplings .....	16
Figure 14. Field Strength Est. using the Voltage Readings of Two Consecutive Samplings.....	16
Figure 15. Pitch and Yaw Orientation Estimation with Tracking Approach which use the Voltage Readings of Two Consecutive Samplings.....	17
Figure 16. Position Data and Estimates using Six (6) Magnetic Sensors.....	18
Figure 17. Dipole Strength and Estimates from using Six (6) Magnetic Sensors .....	18
Figure 18. Pitch and Yaw Data and Estimates of Performance with Six (6) Magnetic Sensors .....	19
Figure 19. Position Data and Estimates using Eight (8) Magnetic Sensors .....	19
Figure 20. Dipole Strength and Estimates from Using Eight (8) Magnetic Sensors .....	20
Figure 21. Pitch and Yaw Data and Estimates of Performance with Eight (8) Magnetic Sensors.....	20
Figure 22. Procedure for Estimation of Location and Estimation of a Moving Magnetic Projectile .....	22
Figure 23. The Sum of the Squares of the Error of “ <i>fminsearch</i> ” and “ <i>nlinfit</i> ” Algorithms (top), The Reported Parameters were the Estimations of the “ <i>nlinfit</i> ” in each case (bottom) .....	23
Figure 24. Location Estimation Accuracy of the Proposed Method .....	23
Figure 25. The Dipole Strength Estimation Accuracy of the Proposed Method .....	24
Figure 26. The Up/Down and Left/Right Attitude Estimation Accuracy of the Proposed Method .....	24
Figure 27. The Pitch and Yaw Estimation Accuracy of the Proposed Method.....	25
Figure 28. Sum of the Squares of the “ <i>fminsearch</i> ” Algorithm.....	26
Figure 29. The Position Estimation Performance of the Proposed Algorithm for Noisy Data.....	26
Figure 30. The Field Strength Estimation Performance of the Proposed Algorithm for Noisy Data .....	27

Figure 31. The Up/Down and Left/Right Attitude Estimation Performance of the Proposed Algorithm for Noisy Data .....	27
Figure 32. The Pitch and Yaw Estimation Performance of the Proposed Algorithm for Noisy Data .....	28
Figure 33. Close up of Pitch and Yaw Estimation Performance of the Proposed Algorithm Between the Sensors .....	28
Figure 34. Position Estimations with “ <i>fminsearch</i> ” (pt-pt), Polynomial Model (model) and Data from High Speed Camera (cam) .....	29
Figure 35. Field Strength Estimation with “ <i>fminsearch</i> ” (pt-pt), and Polynomial Model (model). .....	30
Figure 36. Up/Down and Left/Right Attitude Estimations with “ <i>fminsearch</i> ” (pt-pt), Polynomial Model (model) and Camera (cam) (Positive is up and to the right).....	30
Figure 37. Pitch and Yaw Estimations with “ <i>fminsearch</i> ” (pt-pt), Polynomial Model (model) and Camera (cam) .....	31

This page is intentionally left blank

## 1.0 SUMMARY

The Particulate Mechanics Meso-scale Diagnostics (PMMD) project was to develop multiple, small-scale experimental techniques to measure statistically-expressed, length/time-scale-dependent meso-scale code validation data associated with high-pressure/rate conditions in particulate and granular media. These conditions are generated by the high-speed (10-1,500 m/s) impact of right-circular cylinder, hemi-nose cylinder, or spherical projectiles into specially prepared and instrumented sand beds. This project represents initial steps in establishing AFRL in-house capability for the research and fundamental understanding of high-rate particulate mechanics response at the localized, state response. The ability to quantify and characterize the localization and statistically diverse conditions of dynamic particulate reactions are critical to follow-on research of meso-scale modeling and future, high-fidelity predictive simulation capabilities.

The project had significant leveraging by several AFOSR & AFRL-sponsored collaborations: AORD sponsored research at Osaka, Tohoku and Tsukuba Universities, Japan; Section 219 funded Senior Mechanical Design Student Project by FAMU/FSU College of Engineering, and AFOSR's Summer Faculty Fellowship Program funding to Prof. Ibrahim Tansel, Florida International University.

## 2.0 INTRODUCTION

This three (3) year effort was successful in producing a state-of-the art capability, resulting in the development and implementation of the following: A unique horizontal/vertical precision-ballistics gun system, multiple wave mechanics diagnostics, and two experimental configurations were developed and employed in this research. The diagnostics developed and implemented include a redundant induction-coil system, B-dot (rate change of magnetic field) sensor coils and analysis system for dynamic 5DOF state measurement, a network of flush-mounted surface pressure gages (initial size of  $\phi$  6.35 mm, final size  $\phi$  1.26 mm), fiber optic break wires, colored particulate mechanics layering method, chemical fixing/sectioning of target, and Scanning Electron Microscope (SEM) particle analysis techniques. The two experimental configurations include: 1. High aspect ratio cylindrical target, 2. Low aspect ratio "Papa Bear" type target.

This final report captures the progress and research activities for the last year of the three year effort, while the research of the first two years are found in published works referenced and described in the Background Section below.

## 3.0 BACKGROUND

**Year 1:** The first year had two main thrusts; the first was physical construction of a PMMD gun launch capability with instrumented chamber to accept a suite of diagnostics. The second was experimental efforts with international collaborations via Windows on Science. The effort was captured in the AFRL Technical Report, AFRL-RW-EG-TR-2012-040.

Right-circular ( $\phi$  15 mm x 26 mm) projectiles were fired vertically-downward (150-720 m/s) into acrylic containers ( $\phi$ 80-190 mm) containing quartz Eglin sand. Decreasing container

size increased projectile drag and decreased total penetration depth. Thus, the container is within the projectile's event horizon for at least a portion of penetration path length and some mechanism(s) exists for communication between projectile and container. It was observed that projectile penetration depth is a function of container size when projectiles impact PM in cylindrical containers. Increasing the container size increases the penetration depth, suggesting a feedback mechanism between the container and projectile. Prior research suggests that the PM between the projectile and the container wall is composed of crushed PM (ahead of & adjacent to high-speed projectiles), compacted PM (either due to mechanical compaction prior to the experiment or due to dynamic compaction during the experiment), and as-poured PM. The highly-densified crushed PM is limited to a region within 1.5 projectile diameters of the shot line. Thus, some mechanism must be responsible for communicating stresses between the projectile (and crushed media) and larger containers.

It is proposed, in concurrence with previous researchers, that such stresses are communicated by stress chains. Previous stress chain definitions have been offered as a means to diagnose and understand the stress-carrying structure of the PM fabric. A further definition is therefore proposed to account for "communication chains" composed of multiple chain segments. Such communication chains are distinguished by the ability of the stress at one point or grain to influence the stress level at a remote point along the same communication chain.

Three analytical models were presented which indicate how stresses might be propagated along chains in frictionless PM, PM with friction at the confining forces, and PM with friction at inter-grain interfaces (i.e. between grains in the chain of interest). In practice, each communication chains is likely to encounter a combination of these idealized conditions along their length, but this analysis helps decompose the problem and bound the limiting conditions for various PM types.

**Year 1.5:** This period concentrated on specific diagnostics to begin the quantification of the response to particulate beds being dynamically deformed and intruded by rigid body penetrators. This period of the effort studied the use of redundant induction coil gauges to reduce state estimation uncertainties for moving Lagrangian points (LPs); e.g. discrete points, moving interfaces, projectiles, etc. The technique embeds a small, high-strength magnet at the LP and simultaneously tracks the magnet continuously with five (5) or more induction coils along a single axis of motion. A calibrated coil gauge model is presented as a function of LP position and velocity. The optimized LP state (position and velocity) estimate based upon redundant LP observations allows direct solution for LP velocity; requiring only one differentiation step to obtain acceleration. A specific experimental implementation (Particulate Materials Meso-scale Diagnostics system) is simulated to evaluate and minimize the expected state estimation errors. Induction coil signals with various levels of noise are simulated based upon a prescribed LP state variation with time. The state optimization algorithm attempts to recover the truth state values. Worst-case position estimation errors of  $\pm 0.3\text{mm}$  and velocity estimation errors of  $\pm 0.46\text{ m/s}$  are determined for LPs travelling 0-1,000 m/s at realistic in-lab data noise levels.

**Year 2:** The second year of research, studied the use of an inverse optimization method to extract statistically-distributed grain/meso-scale material property parameters (e.g. Weibull shape parameter used to express the grains' fracture strength) from spatially-integrated Kolsky (Split Hopkinson) Pressure Bar data. The compaction of particulate material samples is simulated with specified grain-scale material properties to create standard axial stress-

engineering strain plots. These data plots are then analyzed to determine the statistically-distributed grain/meso-scale fracture strength properties. An iterative optimization approach is used to converge upon the most-likely material property parameters for comparison with initial simulation values. General stress-strain trends are illustrated as a function of meso-scale properties like variability in particle size and fracture strength and the strengthening effect of crushed nearest-neighbor grains. The complete effort is documented in AFRL-RW-EG-TR-2013-063, “Estimating Statistically-Distributed Grain-Scale Material Properties from Bulk-Scale Experiments”.

**Year 3:** The final year consisted exclusively on advanced diagnostics for the remote sensing of in situ dynamic state of projectiles as affected by the particulate material response. A networked system of induction coils was implemented on small-scale gun-launched projectile experiments. The effort included three components; analytical modeling and representation, experimental implementation and measurements, and optimization for maximizing fidelity of the method and verifying dynamical states. The magnetic tracking diagnostic is based on remotely sensing voltages that a moving, permanently magnetized projectile induces on array of sensing coils. The voltage time history of many coils are recorded digitally as the projectile (scaled penetrator) passes through a sand target. These voltages, together with the precise locations and orientations of each of the sensing coils are used to infer the track of the projectile through the sensor sand target. A conference paper was presented in Oct. 2013 in (Jamison, Keith, K.Kennison, and B.Martin, “Development of a Diagnostic Technique to Track Magnetized Projectiles in Opaque Media) that provided the crux of data for optimization. The abstract is given:

*A new diagnostic method to record the trajectory and orientation of a magnetized projectile traveling through opaque media has been developed. An array of magnetic field sensing coils placed around the projectile flight path produces raw voltage data that, upon analysis, yields the trajectory of the projectile. This paper discusses the theory of operation of the diagnostic, presents the analysis used to convert voltage signals to trajectory information, gives design details of the sensor array, and describes a commissioning test. In this commissioning test, a projectile launched from a 50-mm gun fully penetrated a 35 inch long, right circular cylinder filled with sand. Data from 30 sensing coils were recorded and analyzed to find the trajectory and orientation of the projectile from well before it impacted the opaque material until well after target exit. To test the validity of the method high-speed digital video cameras recorded the penetrator's entry and exit from the sand target. Trajectory and orientations from the magnetic tracking technique compared quite well to the camera observations.*

This task was leveraged with AFRL/RW in-house program experiments and had two additional external efforts:

- A Section 219 funded, Senior Mechanical Design project by FAMU/FSU College of Engineering students called “Tracking Projectiles in Optically Opaque Media”.
- Summer Faculty Fellowship Program (SFFP), Prof. Ibrahim Tansel, Florida International University, “Investigation of the Performance of Magnetic Monitoring System When the State of a Projectile is Estimated from the Voltages of Multiple

Coils”.

The year concluded with an extensive analysis of the gun-launched projectiles into sand media at velocities exceeding 2500 ft/s and a network of the inductive sensing coils being used to estimate state properties. MATLAB software package was the primary tool to take the sensing coil data and develop optimized number, size, location and optimization routines. The optimization effort is described within this report, with the primary contributions being from Prof. Ibrahim Tansel, under the SFFP program.

## **4.0 MAGNETIC SENSOR METHOD**

A magnetic sensor method was developed to monitor the location and orientation of magnetic projectiles. The location and the magnetic fields were estimated by using polynomial models which represented the entire motion. The orientation of the projectile was estimated from the calculated field strength values. Two new tracking methods were proposed to estimate the location and magnetic fields of a magnetic projectile for each sampling instead of the entire motion. Performances of various optimization and curve fitting algorithms of the Matlab were evaluated on the simulated data with the proposed tracking algorithms. Optimum magnetic sensor configuration and the best optimization method were also determined with synthetic data. The performance of the tracking algorithm which integrates the coil voltages to obtain the B-field values, and estimates the location and field strength from them was found the most reliable approach. Optimizations were performed with the Nelder-Mead simplex and nonlinear search algorithms and the estimations of the routine with smallest sum of the squares were used. The results indicated that the proposed tracking method and selected optimization algorithms are very promising for estimation of the position and orientation of the magnetic projectile.

## **5.0 PROCEDURE OF REMOTE MAGNETIC SENSOR**

Information about the penetration characteristics of an object into a material is essential for many engineering and military applications. The difficulty of the experimental data collection depends on the speed of the projectile and transparency of the target. Various methods have been developed with this purpose. However, more accurate, cheaper and convenient methods are in demand. In this study, the performance of a new procedure which uses the multiple magnetic sensors was evaluated on the simulated data.

The researcher mainly used four approaches to monitor the trajectory (and orientation) of projectiles previously [1]. The first approach used optical and visual methods [2-6]. These methods are very effective while the projectile move in a transparent media such as air. The cost of the equipment depends on the desired resolution and speed of the monitored projectile. The information vanishes as soon as the projectile gets into an opaque material. Use of the make or break screens [7-11] was the second approach. The presence of the projectile at different points of the observation zone was detected by using wires or screens to estimate the trajectory and to calculate the speed. However, artifacts disturbing the media such as sand particles leading the projectile may reduce the accuracy of the collected data. The third approach was collection of data with X-ray heads and ground-penetrating radar [10-13]. This approach is capable to monitor the projectile while it is moving in a solid object. However, these instruments are expensive, their sampling frequency may not be fast enough to collect data for fast projectiles

and data cannot be collected if the target is wider than certain limits. The fourth approach is using induction coils [13-15]. A magnet was attached to the projectile and the voltages of the induction coils were monitored while it went through them. The authors showed that the data of multiple induction coils may be used to pinpoint the location with 0.002 m average absolute estimation error when the voltages of highest 5 or more coils were used as long as the external noise stayed below 1% of the coil voltage range.

In this report the following topics will be discussed:

- The theoretical background
- Simulation of the coil voltages
- Tracking the position and field strengths of a magnetic projectile from coil voltages collected simultaneously at the same time (each sampling)
- Results of the tracking from the simulated and experimental data for determination of the following issues:
  - Performances of two tracking methods and effective optimization algorithm(s)
  - Performance of the experimental setups with 6, 8, 10 and 12 magnetic sensors
  - Performance of the selected tracking method and optimization algorithm combination on the simulated, noisy and experimental data

## 5.1 Theoretical Background

In this section modeling the magnetic coils, modeling the motion, calculation of the orientation of the trajectory of a projectile and selected curve fitting approaches are outlined.

### 5.1.1 Modeling the voltage generation at an induction coil with the motion of a dipole:

The voltages of the coils of the magnetic sensors were calculated in the following manner. The induction field of the permanent magnet was calculated first calculated by assuming it to be a simple dipole field. The induction field ( $\vec{B}$ ) was calculated with the following equation:

$$\vec{B} = \nabla \times \vec{A} \quad (1)$$

By considering the strength of the dipole ( $m$ ), the position vector ( $\vec{r}$ ) and the permittivity ( $\mu_0$ ) of the space the following expression was used to calculate the vector potential:

$$\vec{A}(\vec{r}) = \frac{\mu_0}{4\pi} \frac{\vec{m} \times \vec{r}}{r^3} \quad (2)$$

The induction field of the dipole is calculated with the following equation at any point:

$$\vec{B}(\vec{r}) = \frac{\mu_0}{4\pi} \left( \frac{3\vec{r}(\vec{m} \cdot \vec{r})}{r^5} - \frac{\vec{m}}{r^3} \right) \quad (3)$$

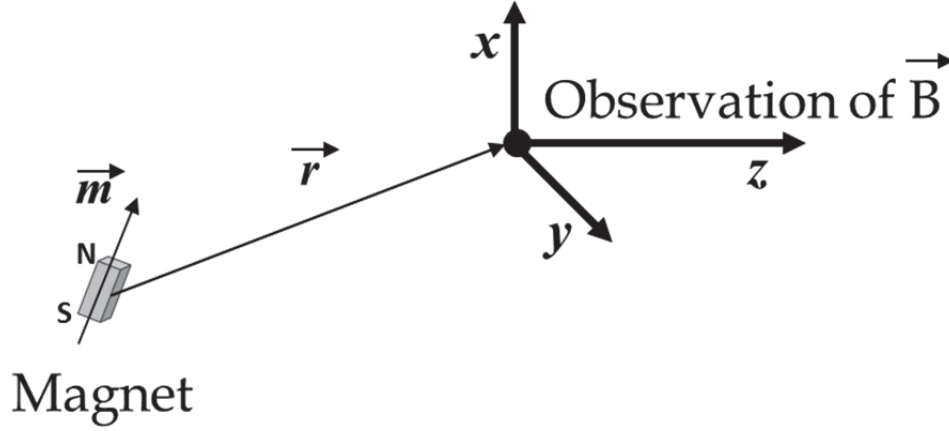


Figure 1. The Dipole and Induction Field at the Origin

The components of the  $(\vec{m}, \vec{r})$  may be represented by the S based on the following relationship:

$$S = \vec{r} \cdot \vec{m} = r_x m_x + r_y m_y + r_z m_z \quad (4)$$

The components of the induction field are calculated by the following when the S term is put into the induction field expression:

$$B_x(r) = \frac{\mu_0}{4\pi} \left( \frac{3r_x S}{r^5} - \frac{m_x}{r^3} \right) \quad (5)$$

$$B_y(r) = \frac{\mu_0}{4\pi} \left( \frac{3r_y S}{r^5} - \frac{m_y}{r^3} \right) \quad (6)$$

$$B_z(r) = \frac{\mu_0}{4\pi} \left( \frac{3r_z S}{r^5} - \frac{m_z}{r^3} \right) \quad (7)$$

The voltage output of a coil which is located in the above induction field is calculated with the following expression.

$$\oint \vec{E} \cdot d\vec{l} = -n \frac{d}{dt} \int_S \vec{B} \cdot d\vec{A} \quad (8)$$

where the  $n$  and  $A$  are the number of turns and coil area, respectively.

### 5.1.2 Modeling the trajectory of a projectile:

To model the trajectory of a projectile two approaches may be used. A simplified method is to represent the components of the trajectory of the magnet with the following polynomial expressions:

$$X(t) = c_{1x} + c_{2x}t + c_{3x}t^2 + c_{4x}t^3 + c_{5x}t^4 \quad (9)$$

$$Y(t) = c_{1y} + c_{2y}t + c_{3y}t^2 + c_{4y}t^3 + c_{5y}t^4 \quad (10)$$

$$Z(t) = c_{1z} + c_{2z}t + c_{3z}t^2 + c_{4z}t^3 + c_{5z}t^4 \quad (11)$$

The components of the dipole were also estimated with the similar expressions:

$$m_x(t) = c_{1mx} + c_{2mx}t + c_{3mx}t^2 + c_{4mx}t^3 + c_{5mx}t^4 \quad (12)$$

$$m_y(t) = c_{1my} + c_{2my}t + c_{3my}t^2 + c_{4my}t^3 + c_{5my}t^4 \quad (13)$$

$$m_z(t) = c_{1mz} + c_{2mz}t + c_{3mz}t^2 + c_{4mz}t^3 + c_{5mz}t^4 \quad (14)$$

The above 6 equations may represent the trajectory and the orientation of the dipole. The 30 parameters of the 6 equations may be calculated by using the Chi-square minimization method. The sampled voltages of all the coils were used for estimation of the parameters.

In this study, the  $X(t)$ ,  $Y(y)$ ,  $Z(t)$ ,  $m_x(t)$ ,  $m_y(t)$ , and  $m_z(t)$  were estimated for each sampling without considering any expression. This approach is very flexible and theoretically represent any motion. On the other hand it is sensitive the noise.

### 5.1.3 Calculation of the orientation of the projectile:

The orientation of the dipole was calculated from the components of the dipole fields with the following expressions:

The up/down attitude,

$$\varphi_{u/d} = \arctan\left(\frac{m_x(t)}{m_z(t)}\right) \quad (15)$$

The left/right attitude,

$$\varphi_{l/r} = \arctan\left(\frac{m_y(t)}{m_z(t)}\right) \quad (16)$$

Pitch,

$$Pitch = \varphi_{u/d} - \arctan\left(\frac{V_x}{V_z}\right) \quad (17)$$

Yaw,

$$Yaw = \varphi_{l/r} - \arctan\left(\frac{V_y}{V_z}\right) \quad (18)$$

Angle of obliquity,

$$AoO = \arctan\left(\frac{\sqrt{V_x^2 + V_y^2}}{V_z}\right) \quad (19)$$

Angle of attack,

$$AoA = \arccos\left(\frac{V_x m_x + V_y m_y + V_z m_z}{\sqrt{V_x^2 + V_y^2 + V_z^2} \sqrt{m_x^2 + m_y^2 + m_z^2}}\right) \quad (20)$$

#### 5.1.4 The Nelder-Mead simplex algorithm:

In this study, the Matlab's "fminsearch" function was used for estimation of the parameters. The "fminsearch" function calculates the parameter by using the Nelder-Mead simplex algorithm [16,17]. The algorithm works without any differentiations. The objective function is minimized with an iterative process. The iterative process creates  $N+1$  vertex for  $N$  dimensions. The steps of the algorithm are order, reflect, expand, contract and shrink the parameters. This algorithm is not the best choice for this application since the boundaries are known. There are other procedures which minimize the objective function much better. However, in the study Nelder-Mead algorithm was selected after the speed, accuracy, reliability and robustness (under the noisy conditions) of several algorithms were compared since it compromised all these criteria.

## 5.2 Experimental Set-up

The optimization process of this paper is to represent and help refine the design of a physical system employed at the Air Force Research Laboratory, Munitions Directorate. A 50-mm diameter, smooth-bore powder gun is used at the Advanced Warheads Experimentation Facility (AWEF) for research of high velocity, rigid-body penetration events. The analytic model and optimization method was specifically designed to represent this physical system of the AWEF. Physical dimensions, magnetic field strengths, and limits (min/max) of the sensor coil network were dictated by that available at the AWEF. The projectiles were magnetized by holding it in a strong magnetic field. A 20 AWG magnet wire with 1,300 turns was used to magnetize the projectile. A 10,000  $\mu\text{F}$  capacitor was charged to 280 V. Later it was discharged to create a strong magnetic field to magnetize the steel projectile. This process and setup were then the starting conditions for the sensor capability, according to the generalized previously given, Eq. (8). Experimental data was collected while the projectile moved among 8 magnetic sensors. Each magnetic sensor had 3 coils.

### 5.3 Simulation Study

In this study, the voltages of the coils of the magnetic sensors were simulated while the projectile moved between 6, 8, 10 and 12 magnetic sensors. The locations of the magnetic sensors at the considered cases are presented in Fig.2. - Fig.5.

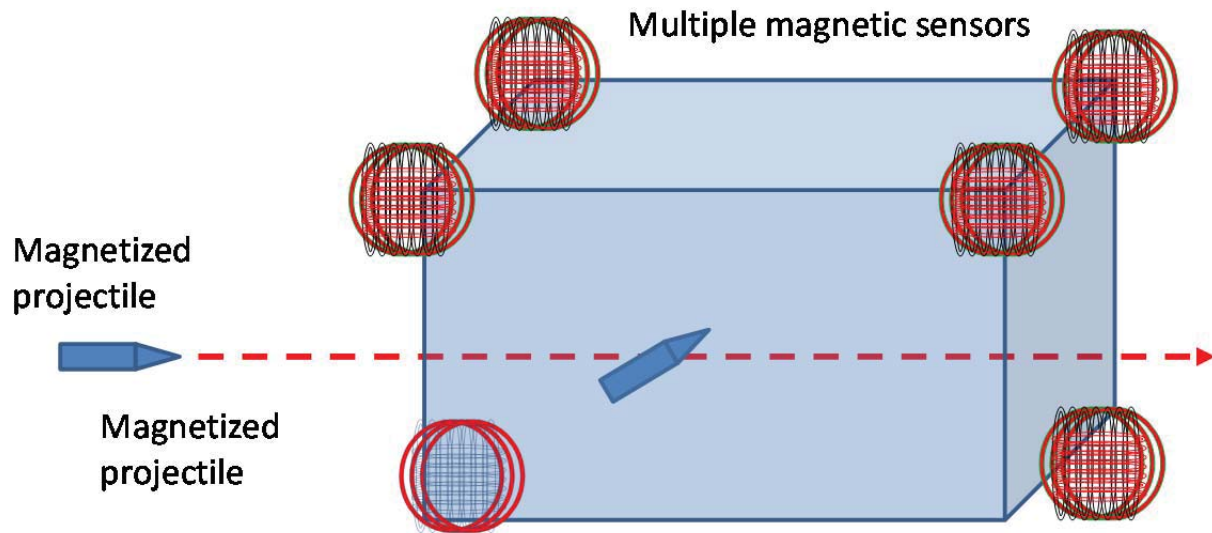


Figure 2. Configuration of Six Magnetic Sensors for Monitoring the Motion of the Projectile

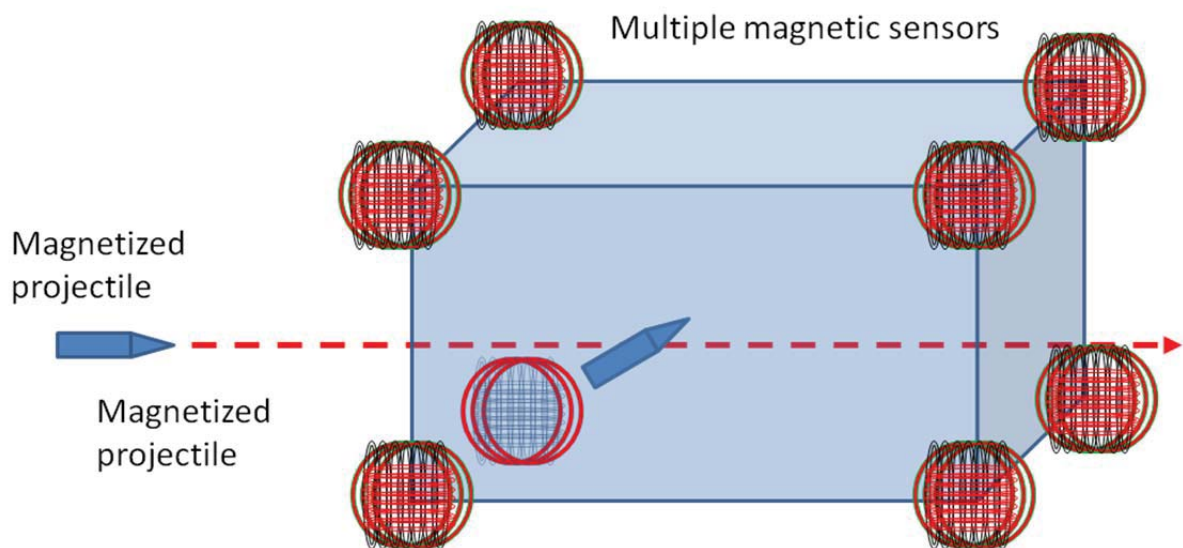
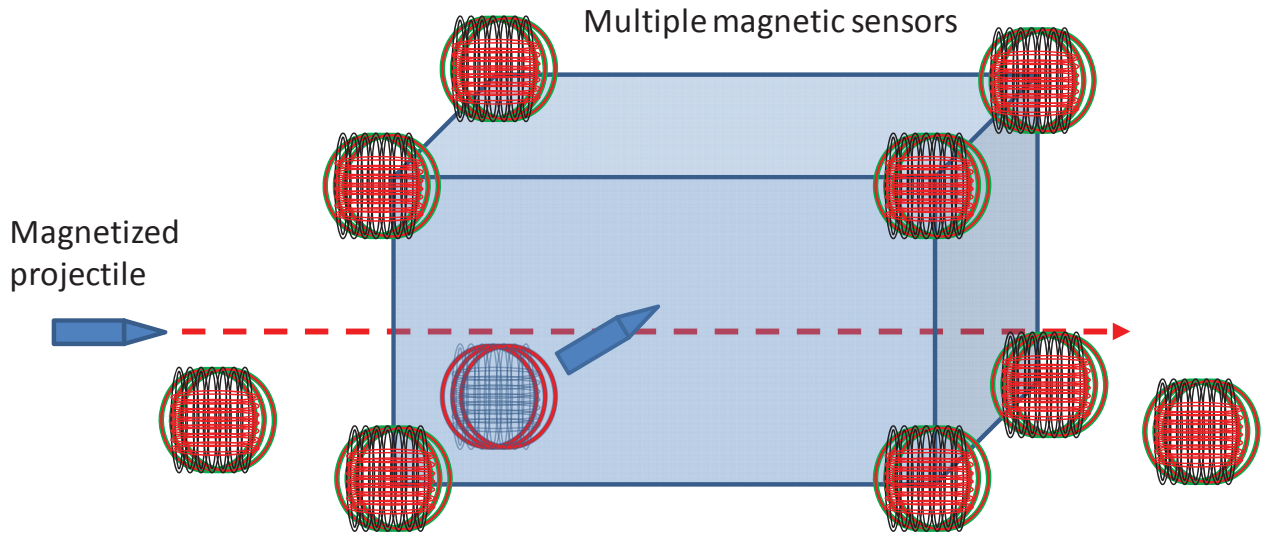
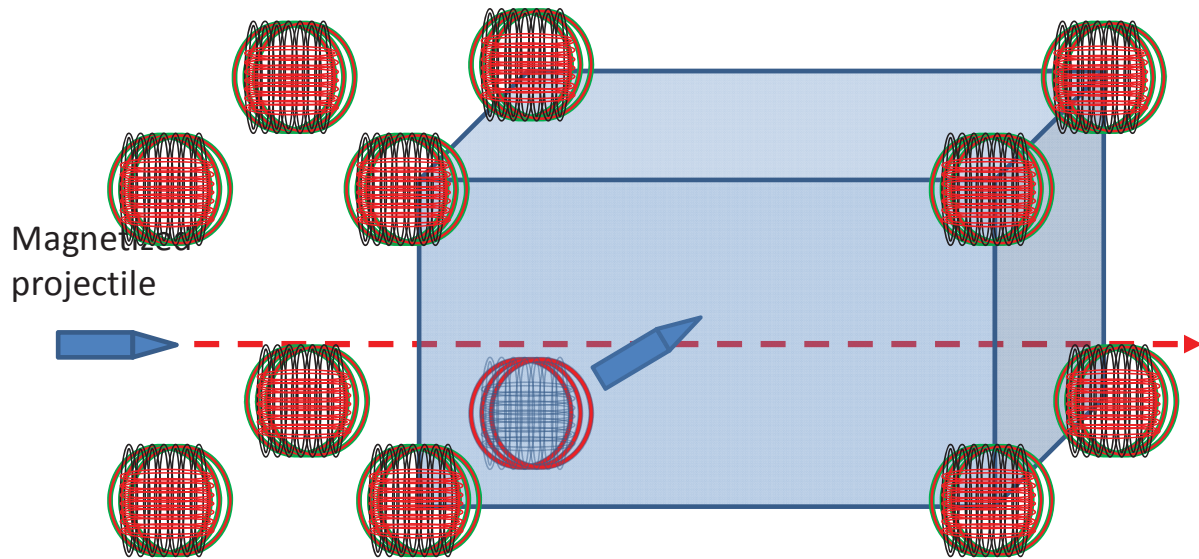


Figure 3. Configuration of Eight Magnetic Sensors for Monitoring the Motion of the Projectile



**Figure 4. Configuration of Ten Magnetic Sensors for Monitoring the Motion of the Projectile**



**Figure 5. Configuration of Twelve Magnetic Sensors for Monitoring the Motion of the Projectile**

The Eq.5 – 7 were used to calculate the strength of the magnetic fields. The voltages of the coils were calculated from the magnetic field strength variation represented in Eq.8. The procedure is presented in Fig.6.

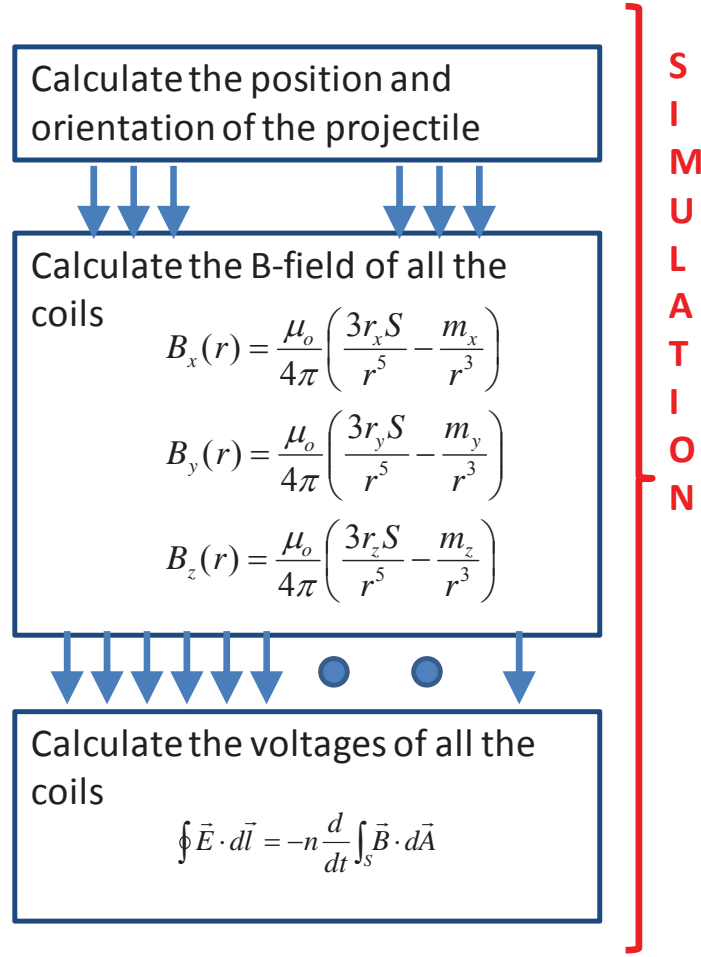


Figure 6. The Procedure used to Generate the Simulation Data

#### 5.4 Proposed Procedure for Monitoring the Motion of a Magnetic Projectile

Electricity is generated when a magnet moves around a properly designed coil. The simulated voltages of the coils were used to estimate the projectile location and the orientation. Two main methods were used. The first method used polynomials to represent the location and field strength. A single fourth order polynomial curve was fit for the entire data set. Thirty (30) parameters of six (6) equations corresponding to the displacement and field strength equations were estimated once. The second method made curve fitting for each simultaneously collected coil voltage data and estimated the location and field strength for each sampling. Furthermore, two approaches were developed for implementation of the second method. One of them estimated position and field strengths from the voltages of all the coils collected at each sampling after the B-field values were calculated. The other approach used the voltages taken at two samplings directly without calculating the B-field values first.

Polynomial modeling of entire motion: this method used the data of all coils acquired during the entire experiment. First the B-field values were calculated by integrating the voltages. The entire motion of the projectile was represented by 6 equations with 5 parameters in each one of them. These equations are given in Eqs. 9-14. Chi-squared method was used for estimation of the parameters. This approach is robust against to noise but do not have the flexibility to identify the sudden changes at the trajectory or orientation. The entry and exit information of the projectile into a target can be obtained accurately if there are no sudden changes – an important consideration and also limitation.

Tracking after B-field values are calculated: The voltages of the coils of the entire data were individually integrated to obtain the B-field values. Later, the position and field strength values were estimated from the B-field values collected at each sampling. The number of estimations was equal to the number of measured voltages for each coil. The procedure is outlined in Fig.7 and Fig.8 when 6 and 8 magnetic sensors were used. The number of coils increased to 30 and 36 when 10 and 12 coils were simulated or used in the experiments.

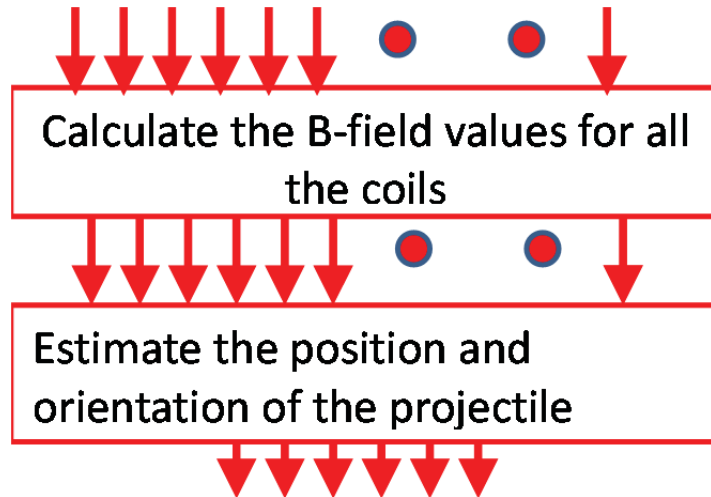


**Figure 7. Proposed Procedure for Estimation of the Trajectory and Orientation of the Projectile**

Tracking directly from the measured voltages: The position and magnetic strength values were estimated from the measured voltages directly for each sampling. In this case, to estimate the voltages, the change of the position and field strength were necessary. The program estimated location and field strength at three consecutive samplings. In addition to the location and field strengths, the rates of these parameters were estimated to calculate the previous and following locations and field strengths. The optimization program calculated the voltages at two consecutive samplings with the estimated parameters and compared with the available data. The parameter estimations were repeated until a good match was obtained between the estimations and the data. Total 12 parameters were estimated. This approach is outlined in Fig. 9.

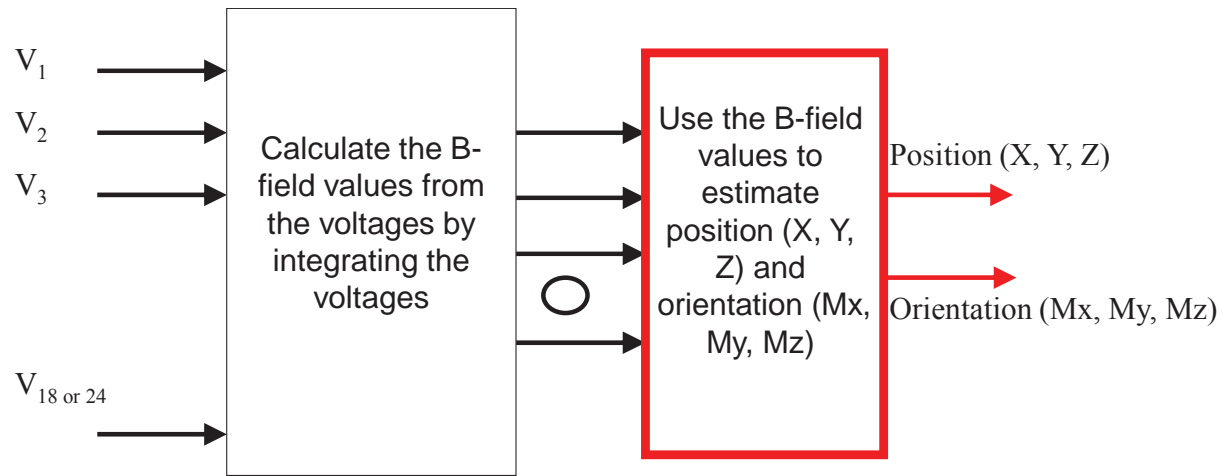


**Figure 8. Proposed Procedure for Estimation of the Position and Orientation**

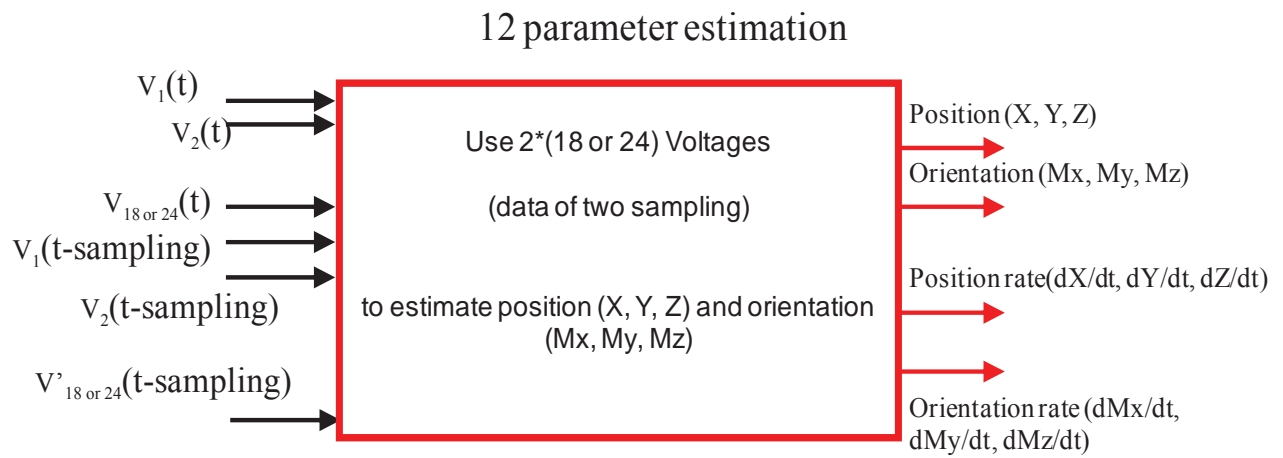


**Figure 9. Proposed Procedure for Estimation of the Position, Field Strength and their Rates to Avoid B-field Estimations**

## 6.0 RESULTS AND DISCUSSIONS

In this section the following topics will be discussed:

- Performance of two tracking approaches which estimated 6 and 12 parameters
- Effect of number and location of the magnetic sensors on the estimations
- Evaluation of the performances of different optimization algorithms and selection of the best procedure for estimation of the parameters
- Performance of the best approach (*fminsearch* + *nlinfit*) on simulated data
- Performance of the best approach (*fminsearch* + *nlinfit*) on experimental data

### 6.1 Performance of two tracking approaches which estimated 6 and 12 parameters

The performance of the tracking method which estimated 6 parameters after B-field values were calculated is demonstrated in Fig.10-12. The position (Fig.10), field strength (Fig.11) and orientation (Fig.12) estimations were accurate when we used the simulated data.

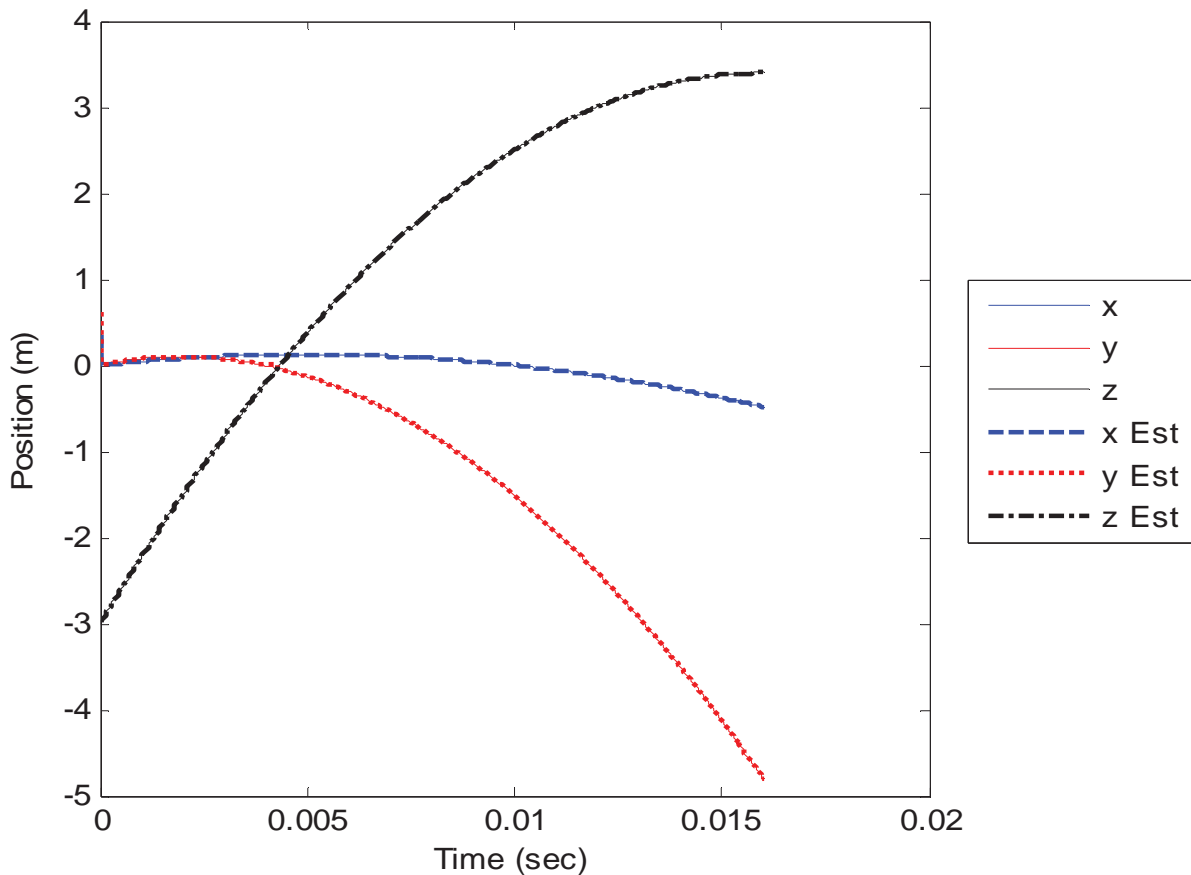


Figure 10. The Position Estimation with Tracking Approach after B-field Estimation

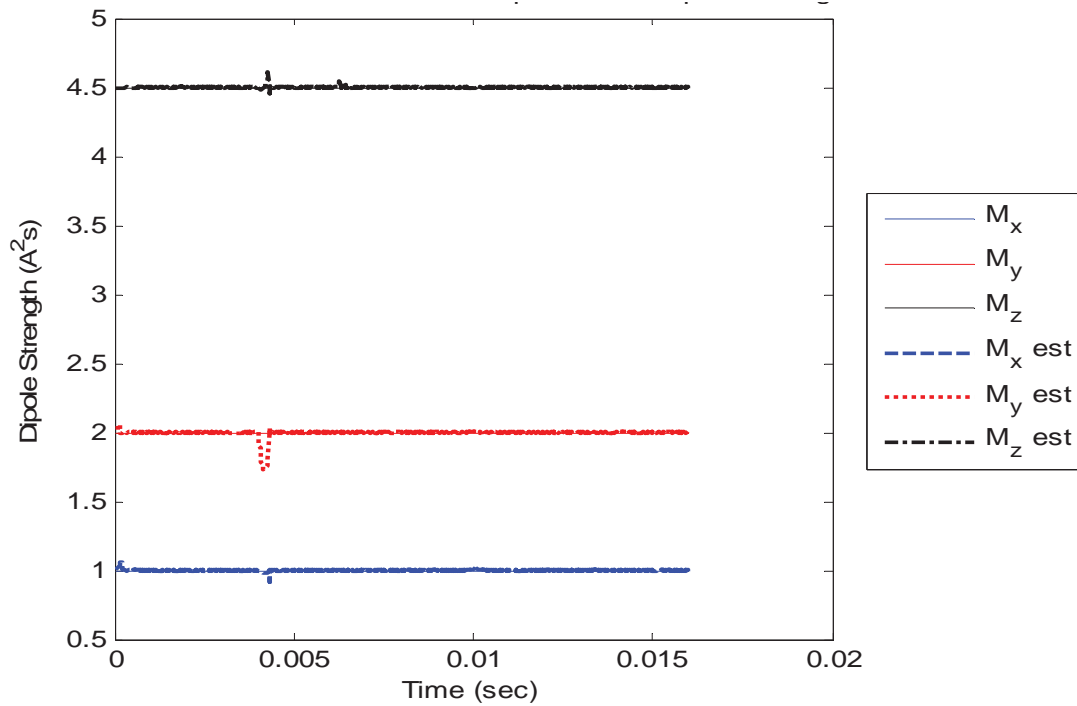


Figure 11. Theoretical and Estimated Vector Components of Dipole Strength

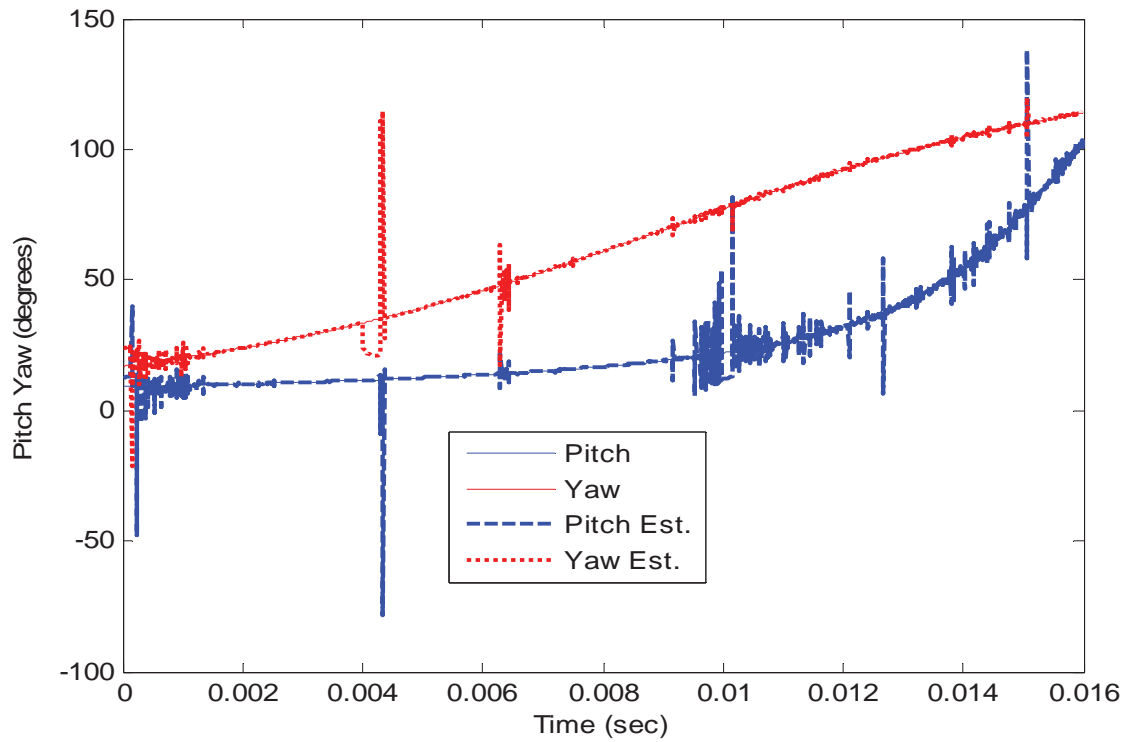
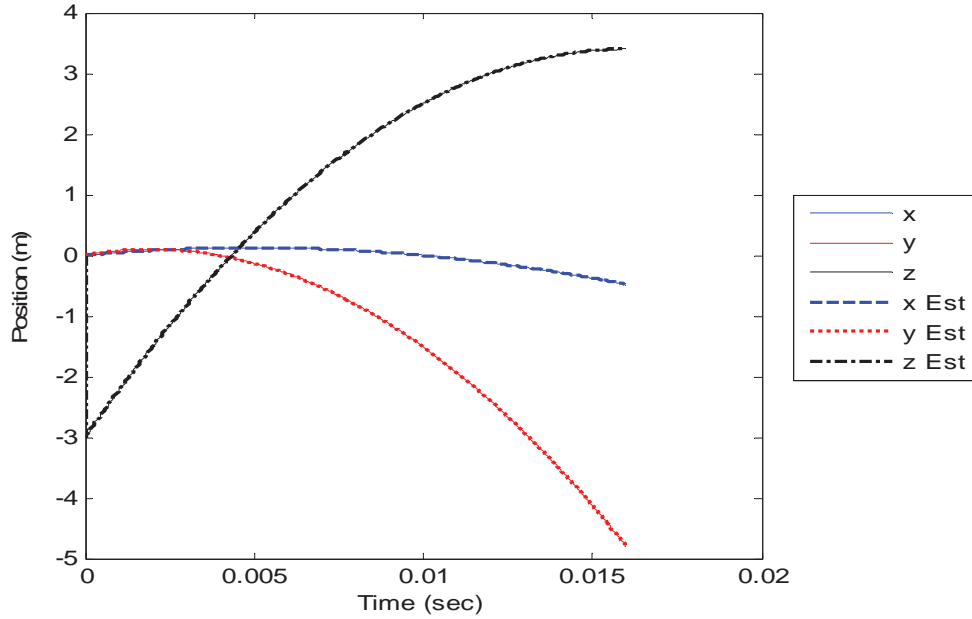
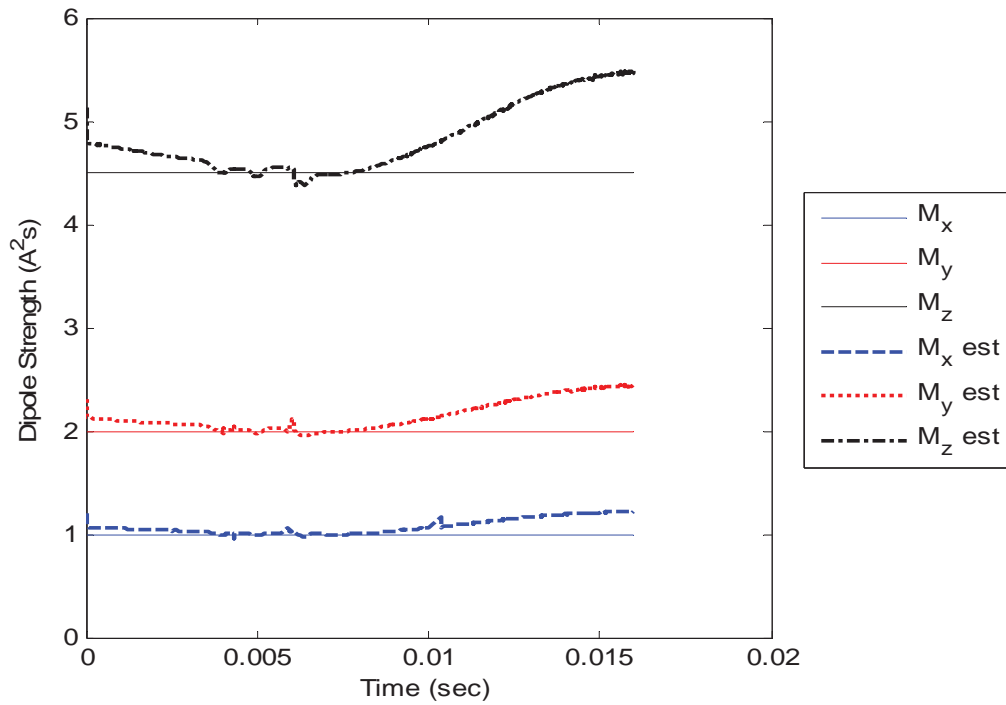


Figure 12. Pitch and Yaw Orientation Estimation with Tracking Approach after B-field Estimation (positive is to the right)

The performance of the tracking method which estimated 12 parameters directly from the voltage measurements of two consecutive sampling presented in Fig.13-15. The position (Fig.13), field strength (Fig.14) and orientation (Fig.15) estimations were reasonable but not as accurate as the first tracking method.



**Figure 13. Position Estimation with Tracking Approach which use the Voltage Readings of Two Consecutive Samplings**



**Figure 14. Field Strength Est. using the Voltage Readings of Two Consecutive Samplings**

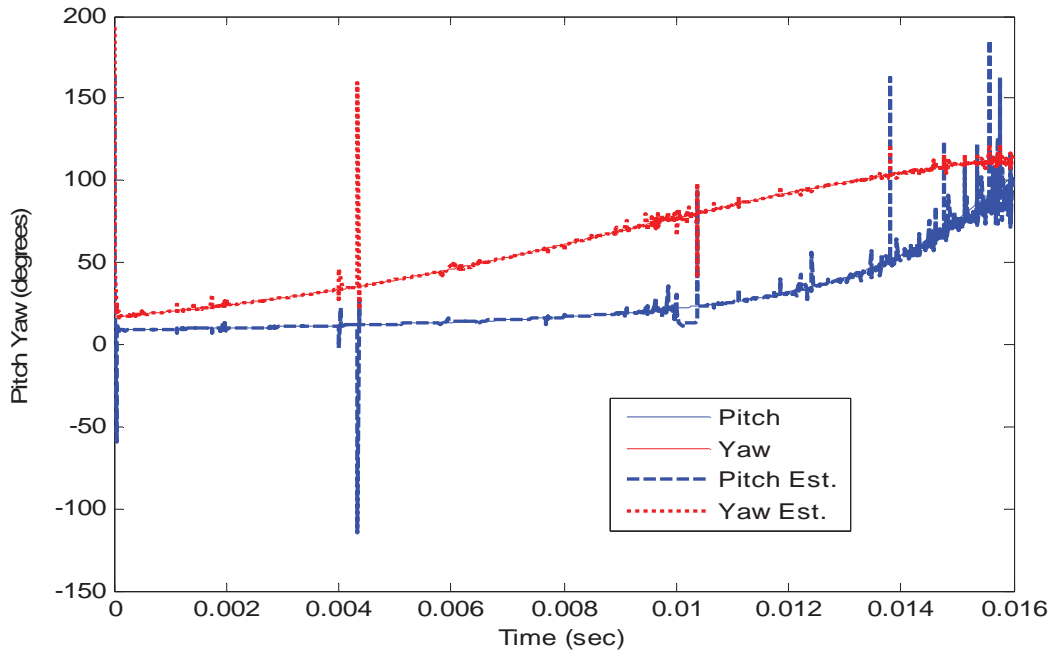


**Figure 15. Pitch and Yaw Orientation Estimation with Tracking Approach which use the Voltage Readings of Two Consecutive Samplings**

Based on the results, the tracking method which estimated 6 parameters from the B-field values was selected for the analysis of experimental data.

## 6.2 Effect of number and location of the magnetic sensors on the estimations

The magnetic sensor configurations given in Figs. 2 to 5 were considered. The coil voltages were simulated at the identical projectile motion and their accuracies were compared. The configuration of 12 magnetic sensors provided too large of a set of equations to solve using the Matlab software and computer system available at the time. It was considered intuitively “better” to use the data of the magnetic sensors which were closest to the projectile. The effective monitoring volume for the tests was doubled with this arrangement. The 10 magnetic sensor configuration of Fig.4 gave the minimum estimation error. By considering simplicity and symmetry, the 6 and 8 magnetic sensor combinations were also studied. The position and dipole strength estimations of both approaches also excelled in different categories, as seen in Fig.16 through Fig. 21. This data is also tabulated in Table 1 and Table 2. Based on the results, eight (8) magnetic sensor configuration was found more preferable.

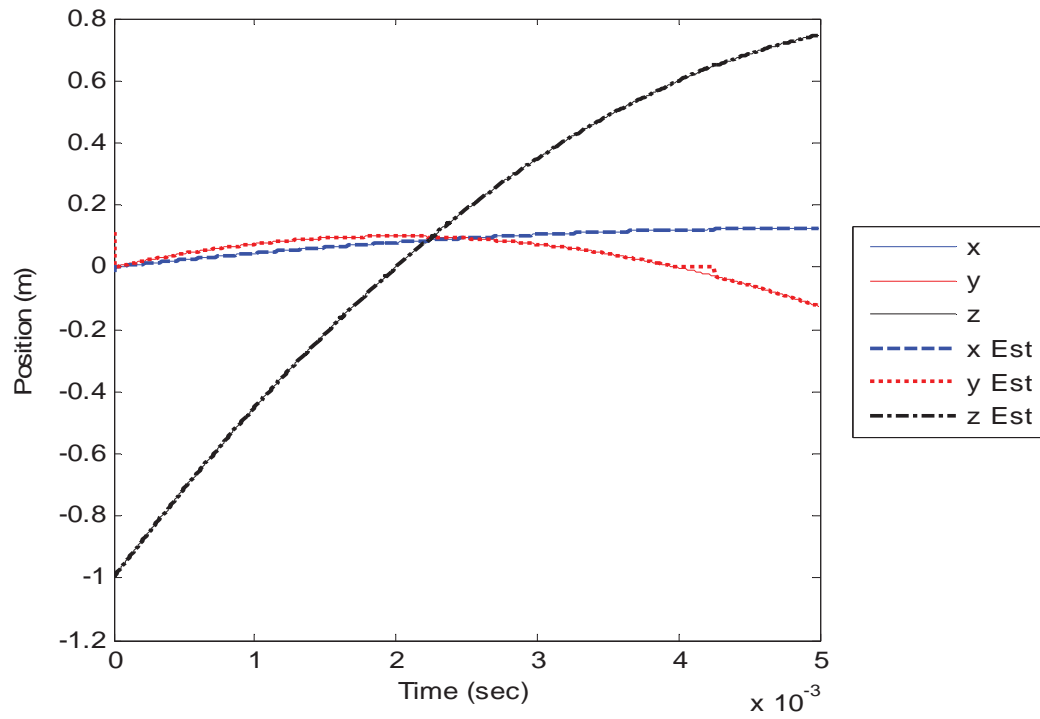


Figure 16. Position Data and Estimates using Six (6) Magnetic Sensors

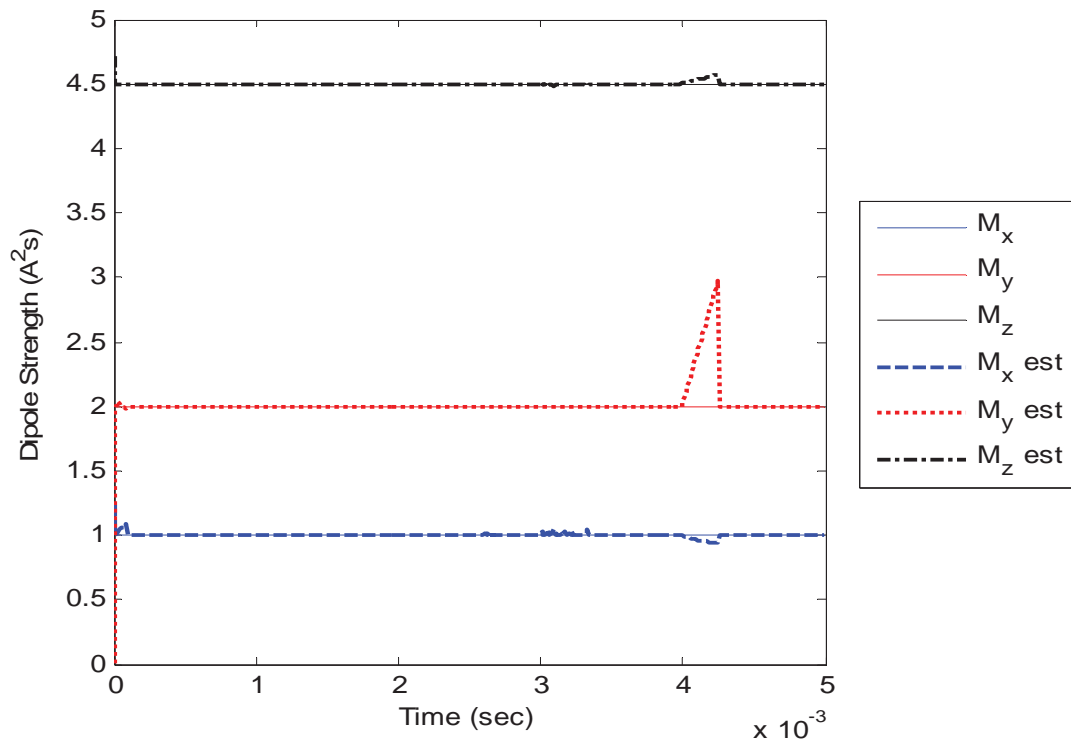
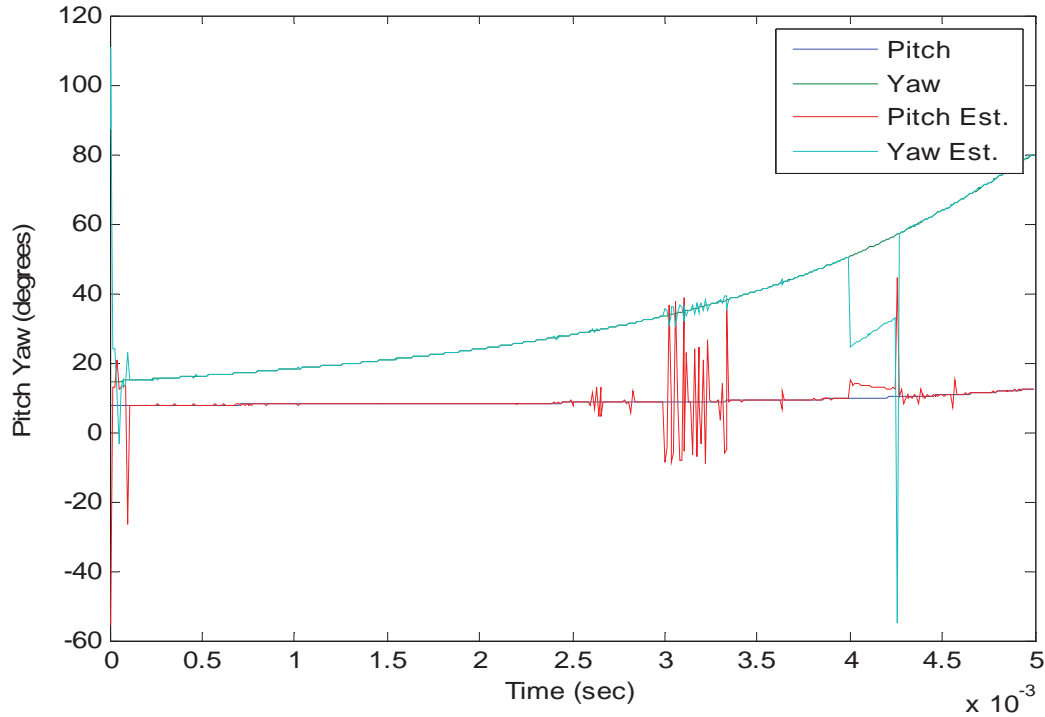
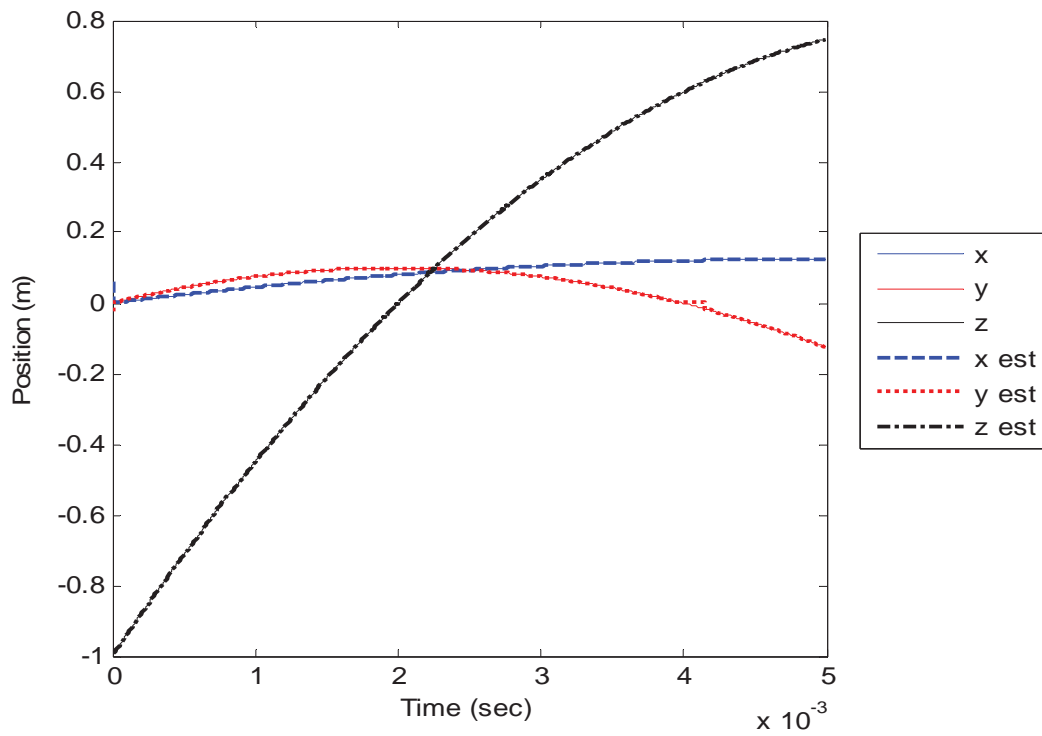


Figure 17. Dipole Strength and Estimates from using Six (6) Magnetic Sensors



**Figure 18. Pitch and Yaw Data and Estimates of Performance with Six (6) Magnetic Sensors**



**Figure 19. Position Data and Estimates using Eight (8) Magnetic Sensors**

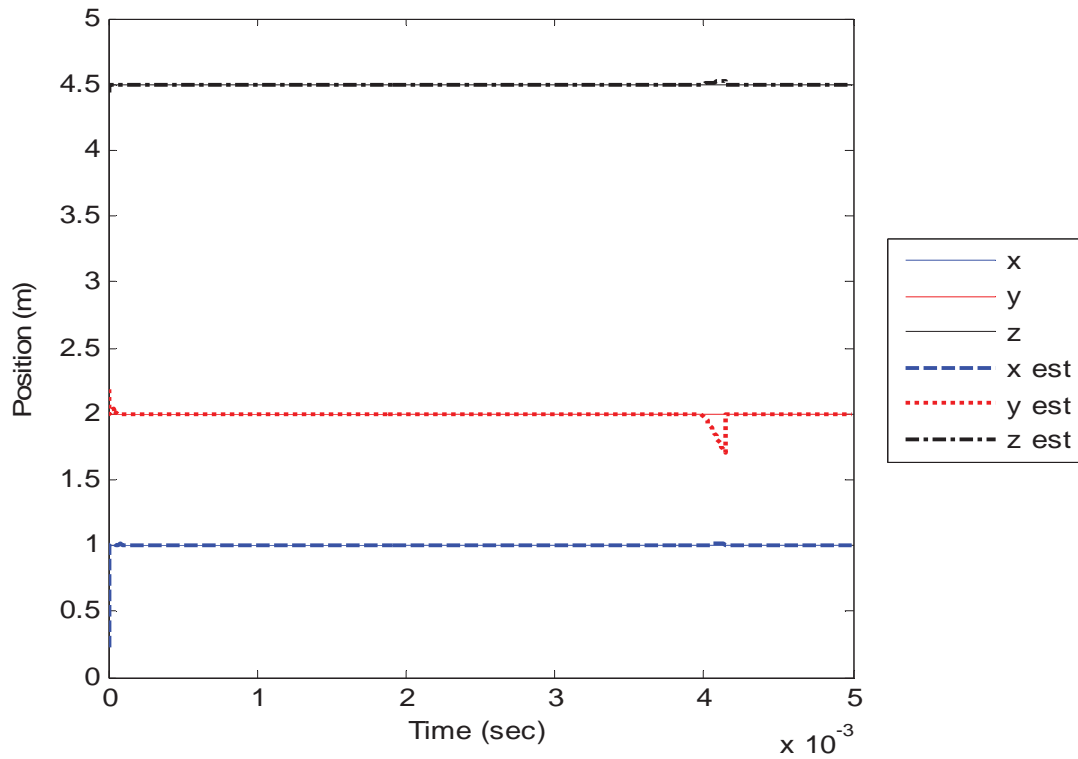


Figure 20. Dipole Strength and Estimates from Using Eight (8) Magnetic Sensors

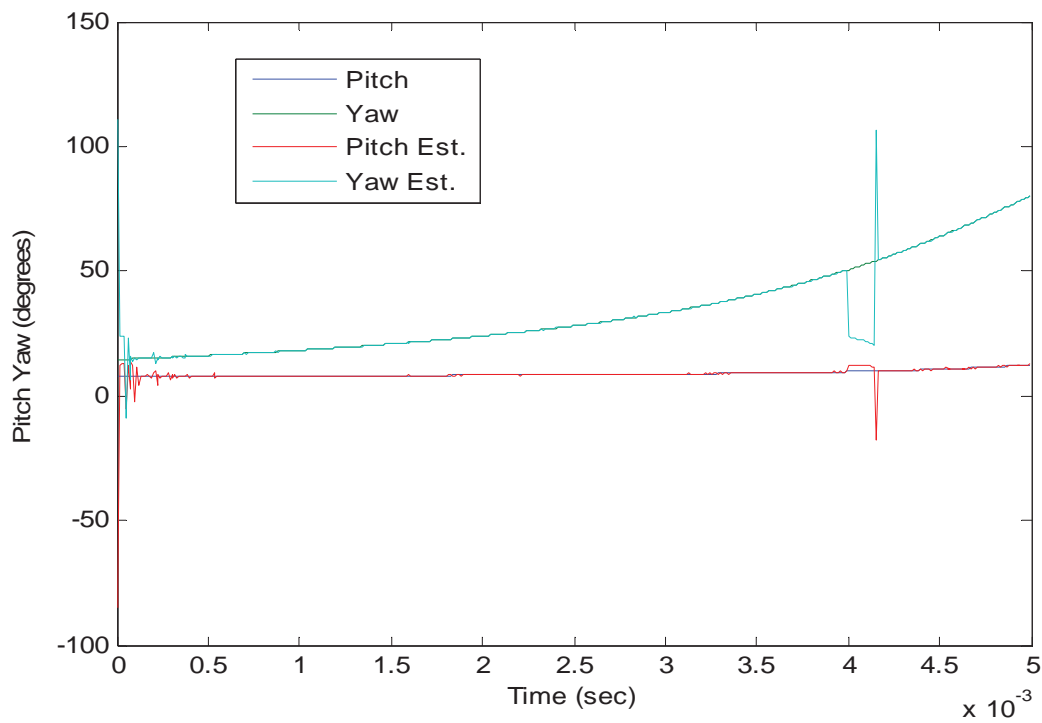


Figure 21. Pitch and Yaw Data and Estimates of Performance with Eight (8) Magnetic Sensors

**Table 1. The Position Estimation Accuracy of the Proposed Procedure for the X and Z Axes**

Considered case			18 coils of 6 magnetic sensors	24 coils of 8 magnetic sensors
Position estimation accuracy	X axis	Average	0.21 mm	0.16 mm
		Max	14.7 mm	61.6 mm
		Sum of Sq	436 mm <sup>2</sup>	3808 mm <sup>2</sup>
	Z axis	Average	0.20 mm	0.027 mm
		Max	7.4 mm	8.33 mm
		Sum of Sq	468 mm <sup>2</sup>	70 mm <sup>2</sup>

**Table 2. The Components of Dipole Strength along the X and Z Axes**

Considered case			18 coils of 6 magnetic sensors A <sup>2</sup> s	24 coils of 8 magnetic sensors A <sup>2</sup> s
Position estimation accuracy	X axis	Average	0.0041663	0.0020533
		Max	0.23596	0.76909
		Sum of Sq	0.13745	0.59442
	Z axis	Average	0.0028113	0.00072312
		Max	0.21612	0.067831
		Sum of Sq	0.097382	0.010275

### 6.3 Evaluation of the performances of different optimization algorithms and selection of the best procedure for estimation of the parameters

Different optimization and curve fitting algorithms of the Matlab toolboxes were used. Among all the algorithms the “*fminsearch*” - Nelder-Mead simplex algorithm gave the most reliable results with reasonable accuracy.

The nonlinear search (*nlinfit*) gave the most accurate results when it worked; however, it was not as reliable as the “*fminsearch*.”. The algorithms of “*fsolve*,” simulated annealing, genetic

algorithm, “*patternsearch*,” algorithms were also used; however, they were not found reliable when the projectile motion was complex and/or the data was noisy.

Based on the results, the best approach was found using the “*fminsearch*” - Nelder-Mead simplex algorithm to make the initial estimations for 6 parameters (location and field strength). Later, these parameters were given to the “*nlinfit*” – nonlinear search algorithm to improve the accuracy of the estimations. However, when we worked with the noisy and experimental data the estimations of the nonlinear search algorithm was worse than the “*fminsearch*” algorithm. So, the developed program compared the sum of the squares of the estimation of the “*fminsearch*” and “*nlinfit*” for each sampling and reported the estimated parameters of the one which has the lowest sum of the squares. This algorithm is presented in Fig.22.

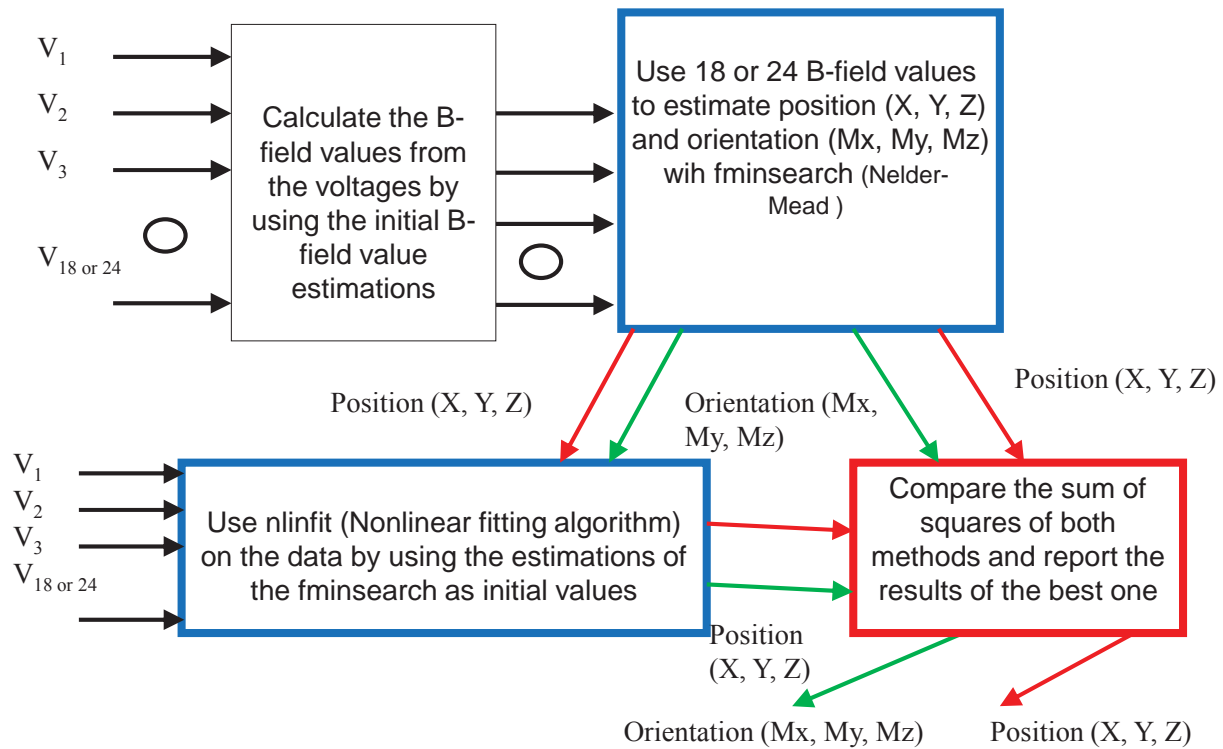


**Figure 22. Procedure for Estimation of Location and Estimation of a Moving Magnetic Projectile**

### 6.3.1 Performance of the best approach (*fminsearch* + *nlinfit*) on simulated data:

The performance of the proposed algorithm in Fig.22 was evaluated on the simulated data when the projectile made complex and very quick maneuvers. The “*fminsearch*” made the initial estimations, the *nlinfit* drastically improved them (Fig.23). The algorithm reported the result of the “*nlinfit*” each case (Fig.23). The average absolute position error was 0.074238 mm (Fig.24). The field strength (Fig.25), attitude (Fig.26), and Pitch/yaw (Fig.27) estimation accuracies were also excellent.

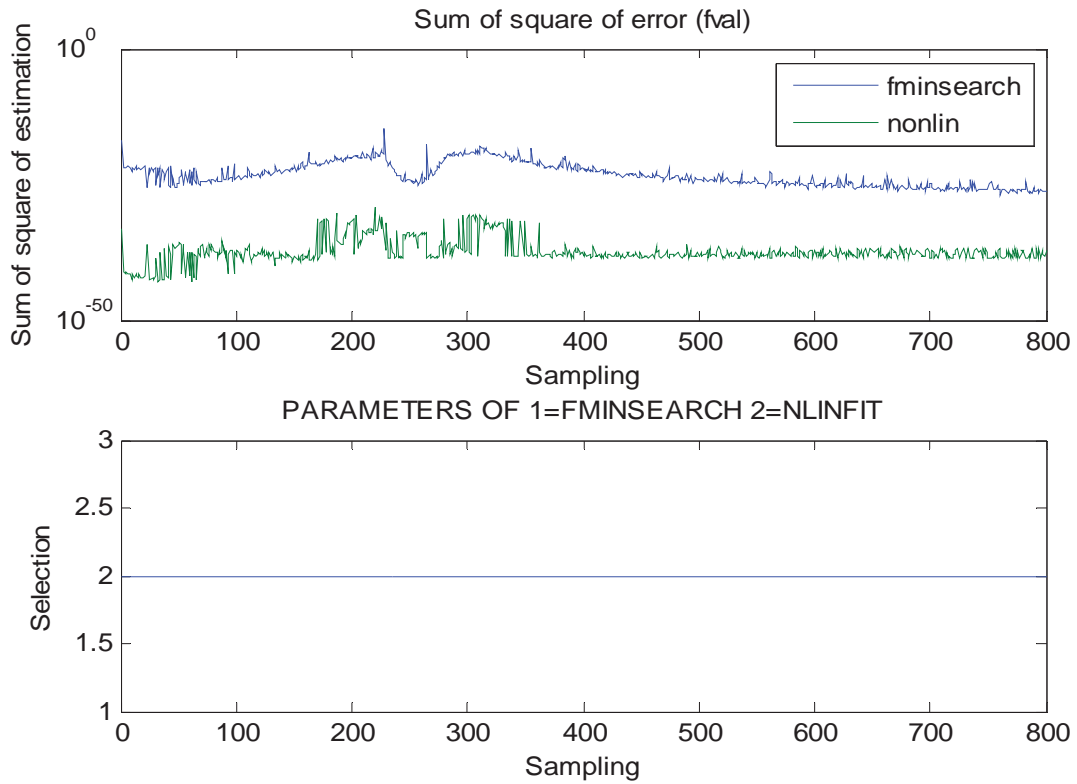


Figure 23. The Sum of the Squares of the Error of “*fminsearch*” and “*nlinfit*” Algorithms (top), The Reported Parameters were the Estimations of the “*nlinfit*” in each case (bottom)

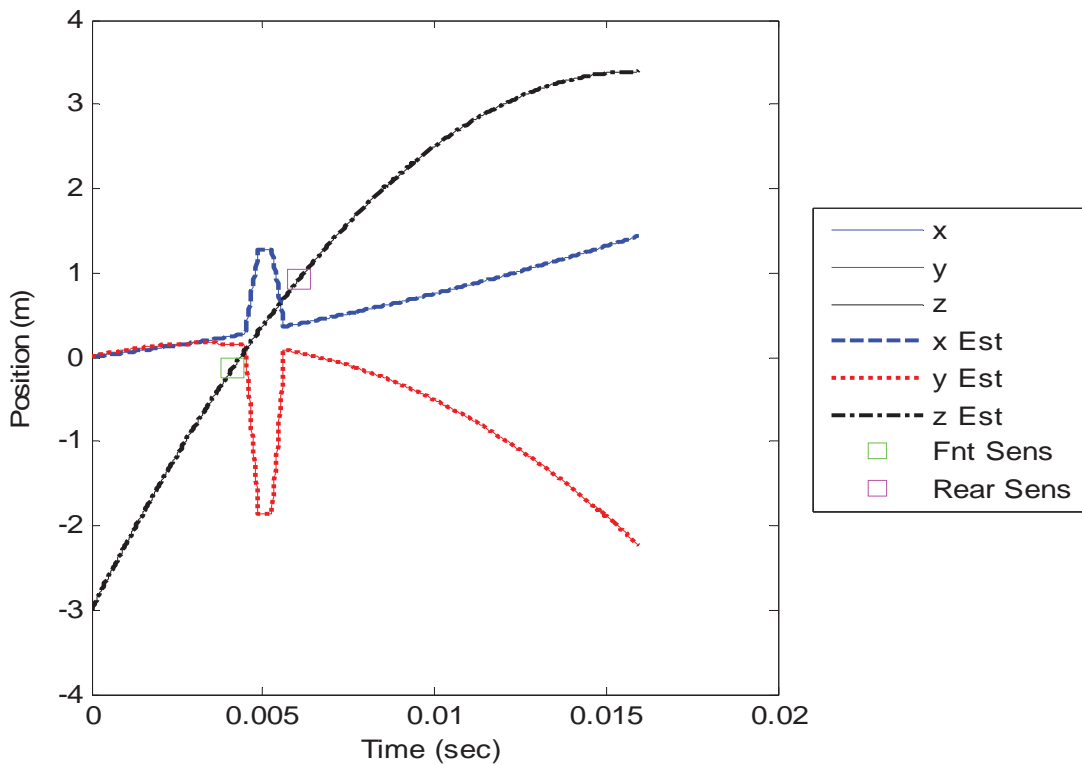


Figure 24. Location Estimation Accuracy of the Proposed Method

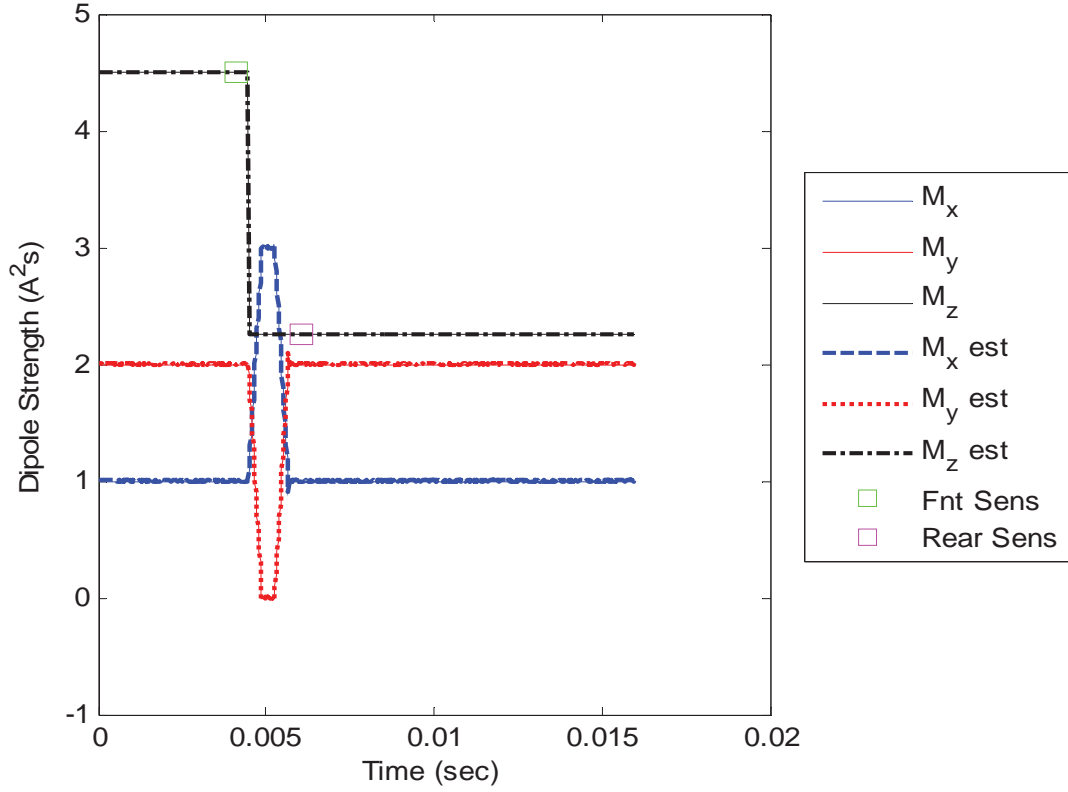


Figure 25. The Dipole Strength Estimation Accuracy of the Proposed Method

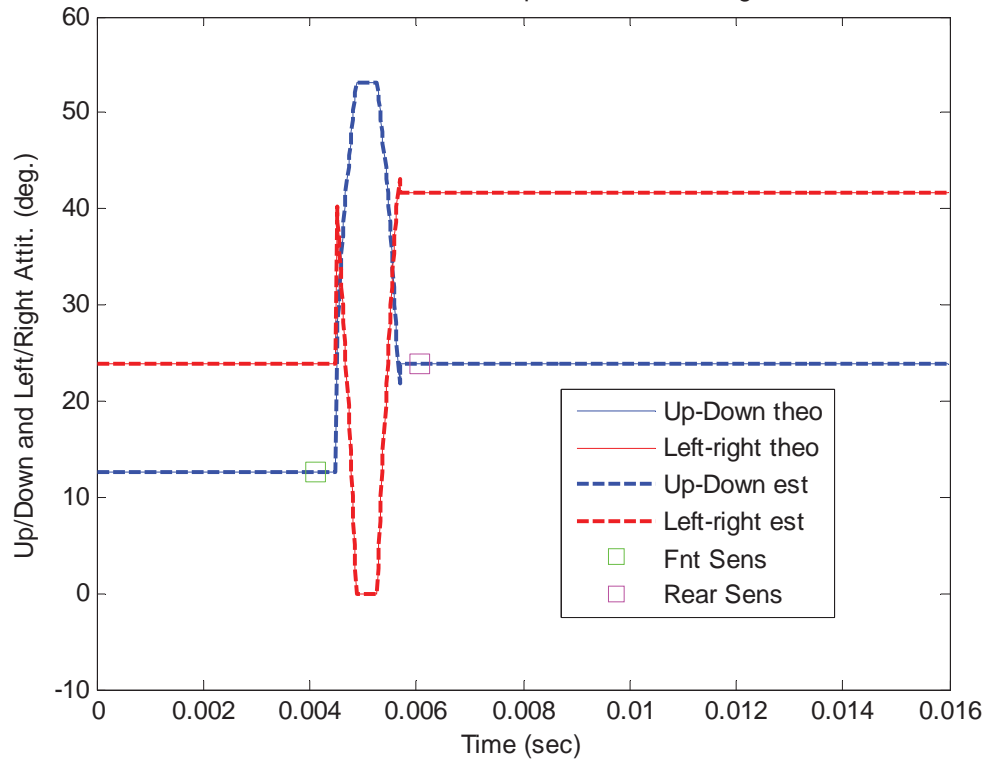
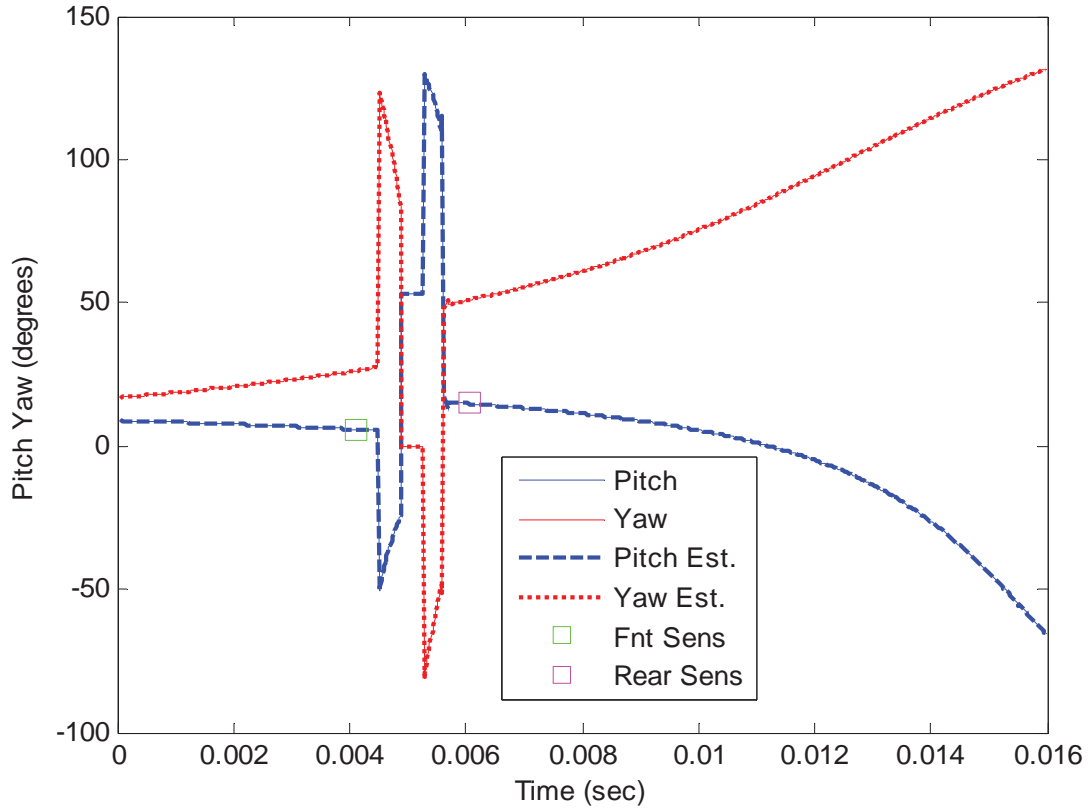


Figure 26. The Up/Down and Left/Right Attitude Estimation Accuracy of the Proposed Method



**Figure 27. The Pitch and Yaw Estimation Accuracy of the Proposed Method**

The performance of the proposed method suffered when 0.1% noise was added to the simulated coil voltages. The proposed algorithm in Fig. 22 preferred the parameter estimations of the “*fminsearch*” since the “*nlinfit*” did not have better sum of the square values (Fig. 28) in almost every case. The position (Fig. 29), field strength (Fig. 30), attitude (Fig. 31) and pitch/yaw (Fig. 32 and 33) estimations were reasonable test volume surrounded by the magnetic sensors but not as good as the no-noise case (Figs. 24-27). Even though, the estimations fluctuated when the projectile moved very fast, the entry and exit estimations (Fig. 33) were very consistent and acceptable at many applications.

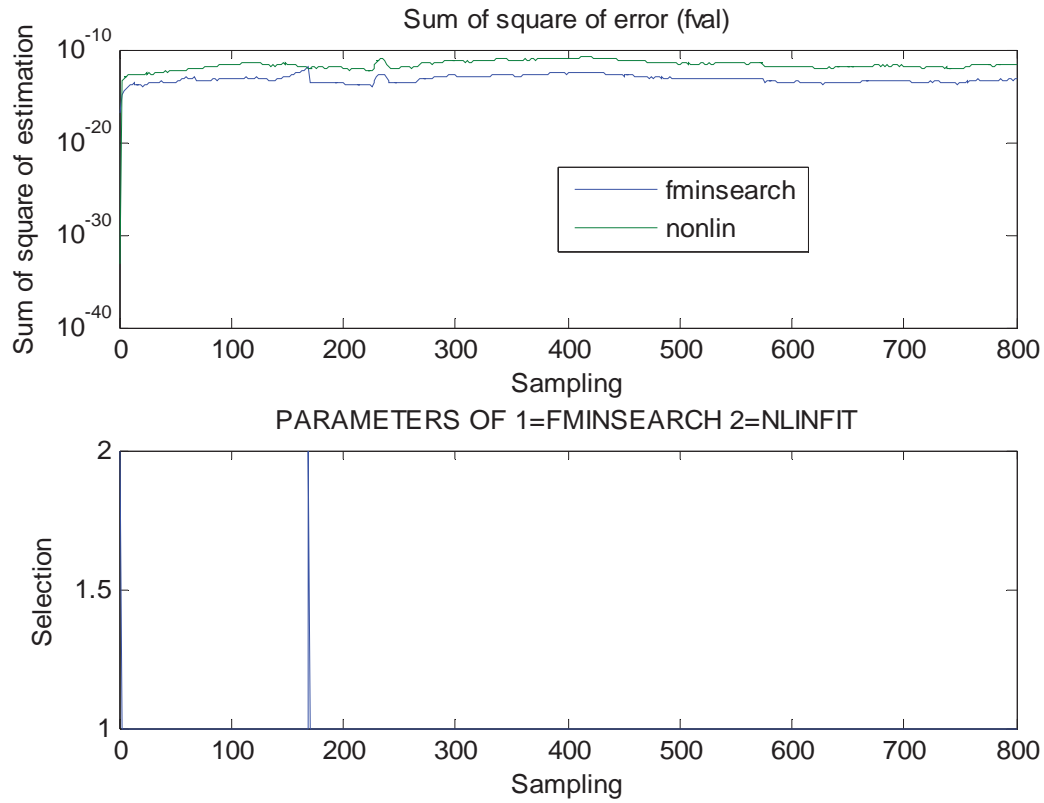


Figure 28. Sum of the Squares of the “*fminsearch*” Algorithm

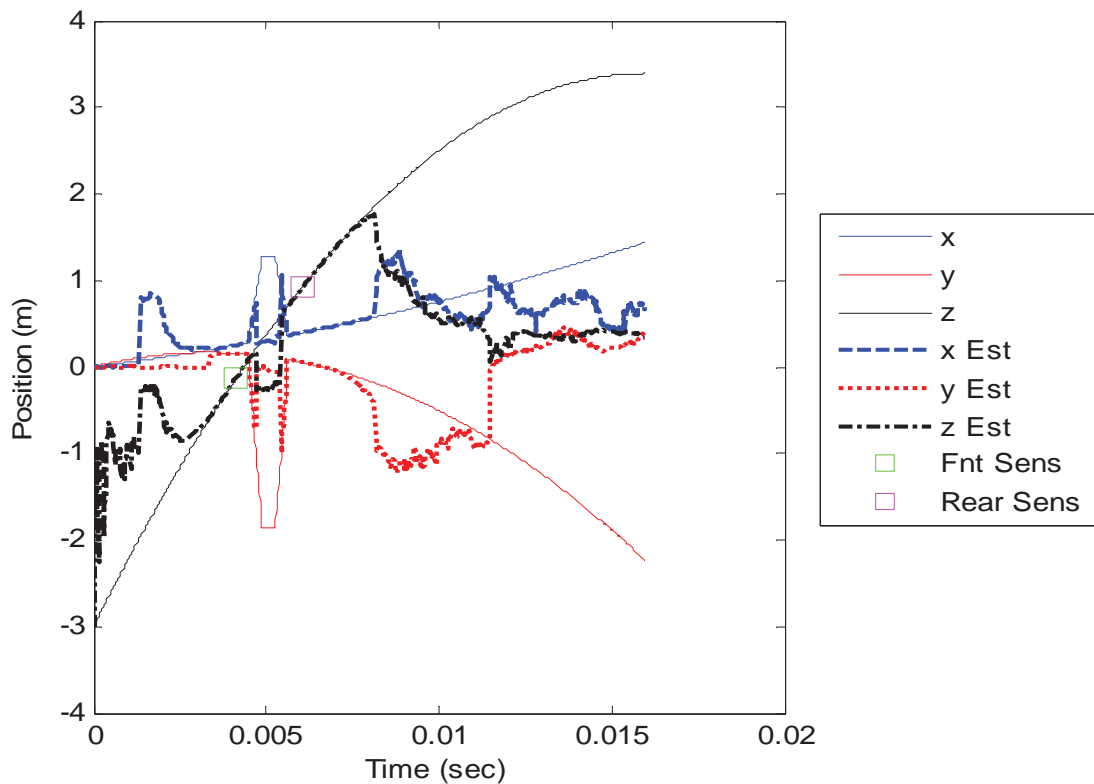
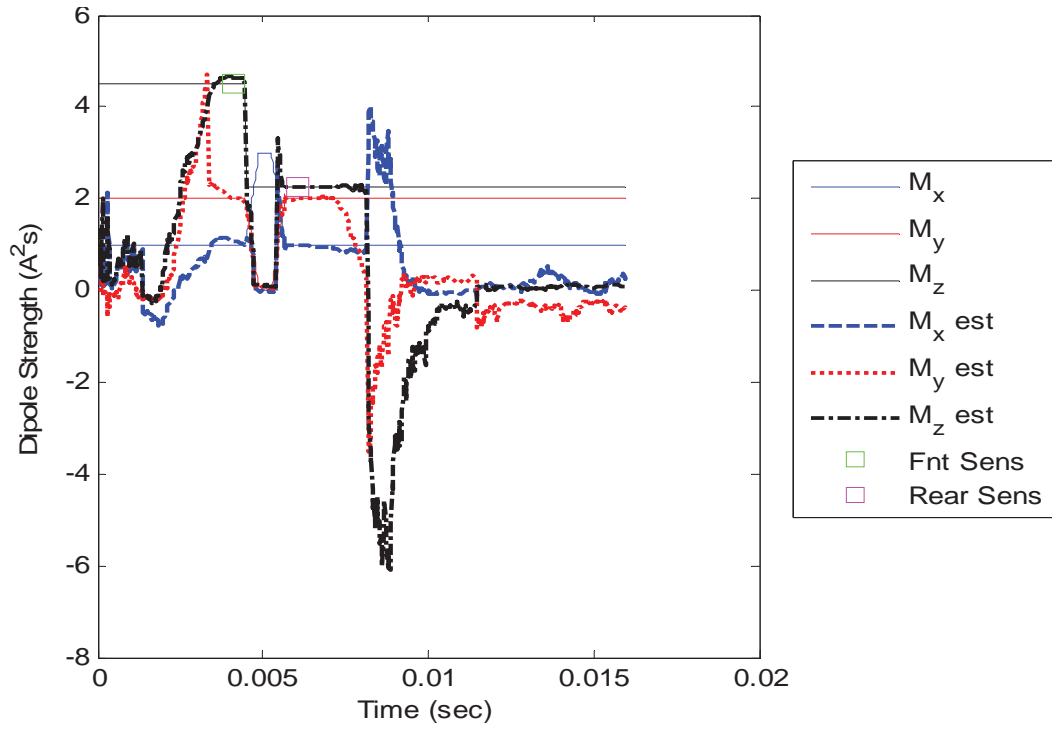
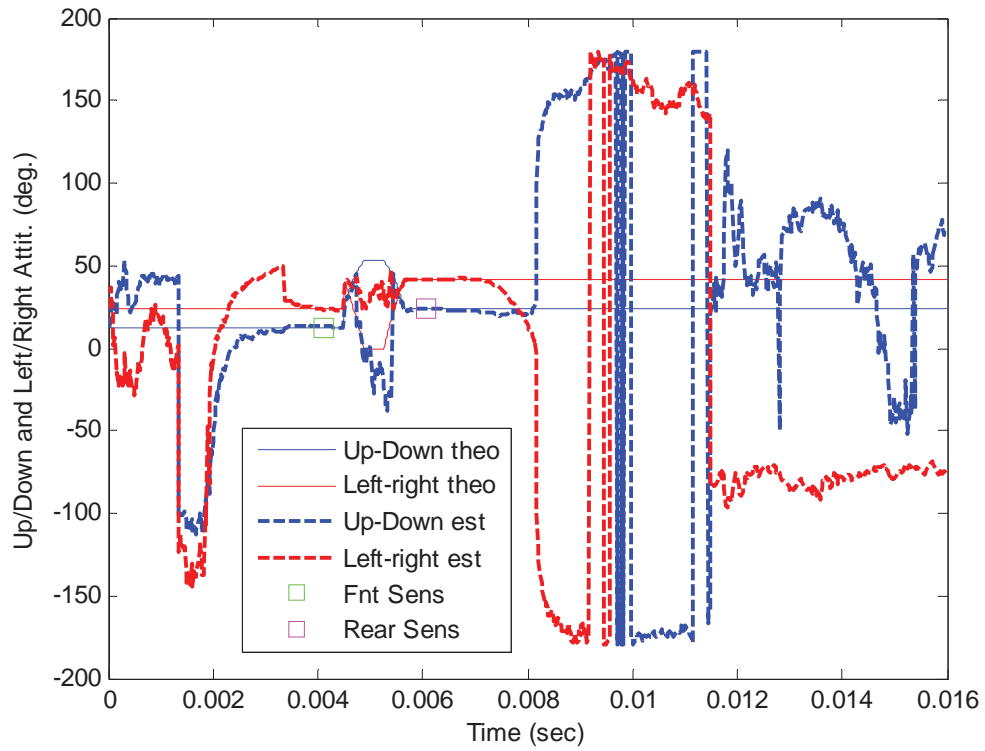


Figure 29. The Position Estimation Performance of the Proposed Algorithm for Noisy Data



**Figure 30. The Field Strength Estimation Performance of the Proposed Algorithm for Noisy Data**



**Figure 31. The Up/Down and Left/Right Attitude Estimation Performance of the Proposed Algorithm for Noisy Data**

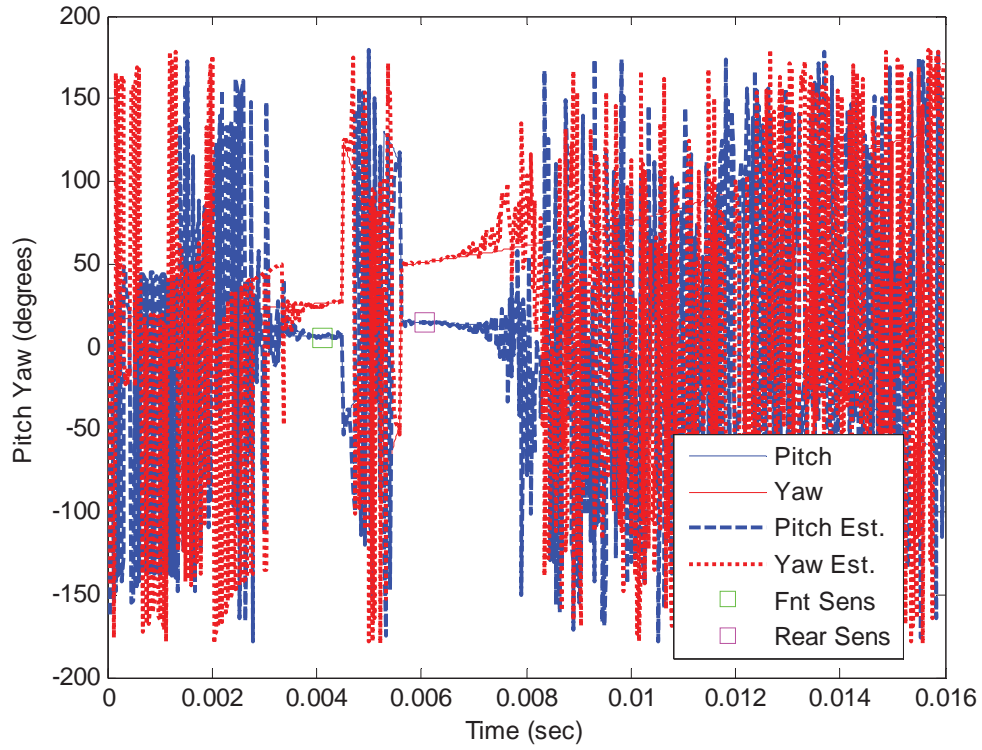


**Figure 32. The Pitch and Yaw Estimation Performance of the Proposed Algorithm for Noisy Data**

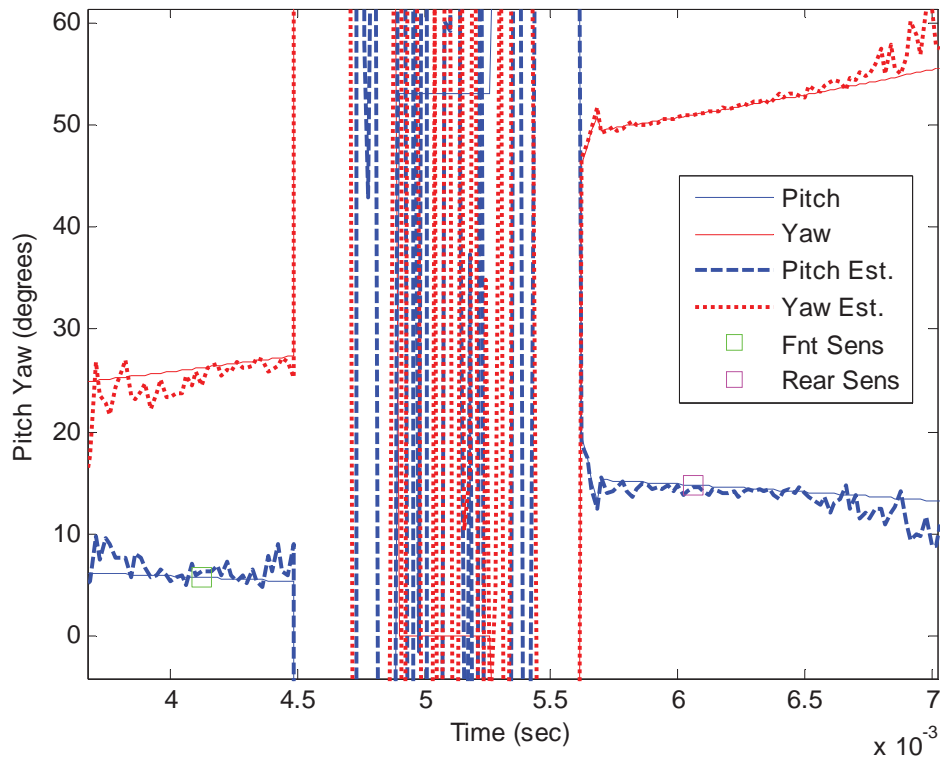


**Figure 33. Close up of Pitch and Yaw Estimation Performance of the Proposed Algorithm Between the Sensors**

### 6.3.2 Performance of the best approach (*fminsearch* + *nlinfit*) on experimental data:

The proposed algorithm in Fig.23 selected the parameter estimations of the “*fminsearch*” algorithm after it compared the sum of the squares of both approaches. Briefly, all the experimental data was analyzed by using the “*fminsearch*” algorithm. For the experimental data the performances of the polynomial model, estimations of the “*fminsearch*” algorithm and the results of the analysis from the images of the high speed cameras were compared. The position estimations (Fig.34) of all the methods were very consistent. The field strength estimations of the polynomial model and “*fminsearch*” were also very close to each other and had the same trend (Fig.35). Similarly, the attitudes (Fig.36) and pitch/yaw (Fig.37) plots of three approaches gave similar results.

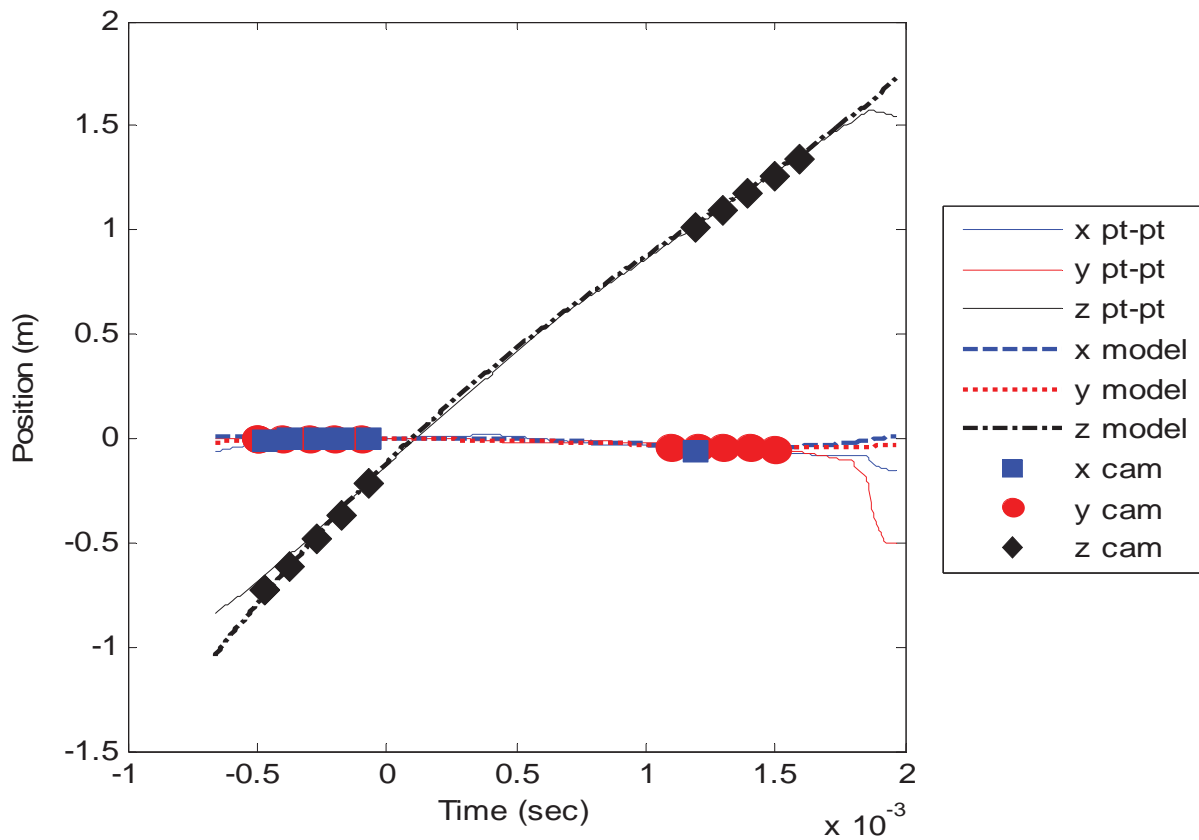


Figure 34. Position Estimations with “*fminsearch*” (pt-pt), Polynomial Model (model) and Data from High Speed Camera (cam)

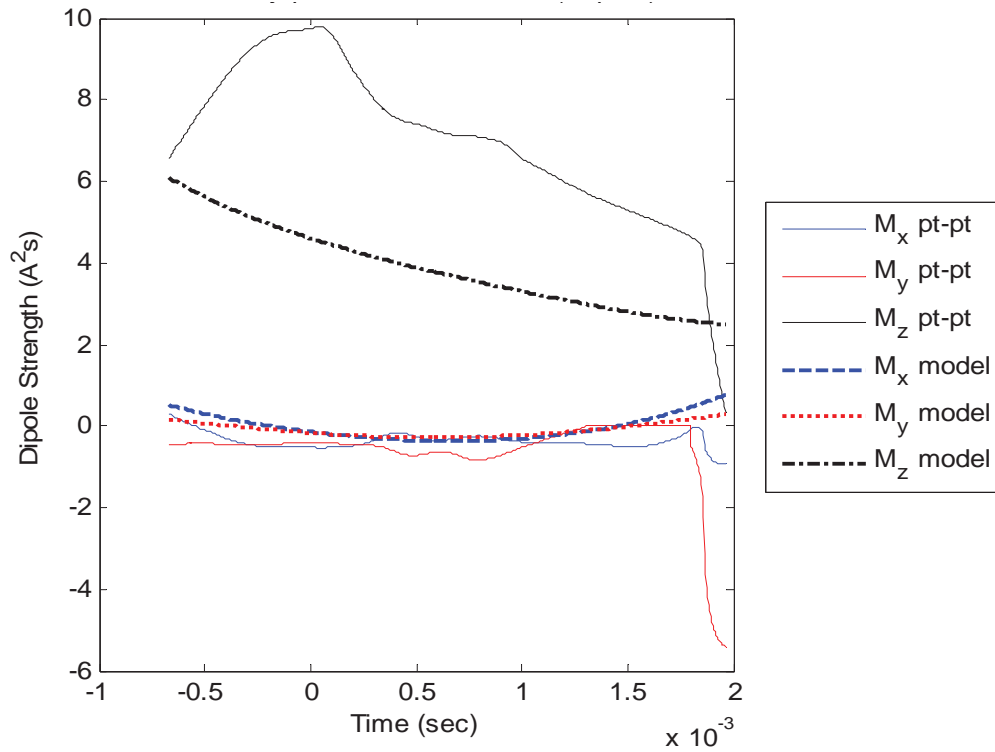


Figure 35. Field Strength Estimation with “*fminsearch*” (pt-pt), and Polynomial Model (model).

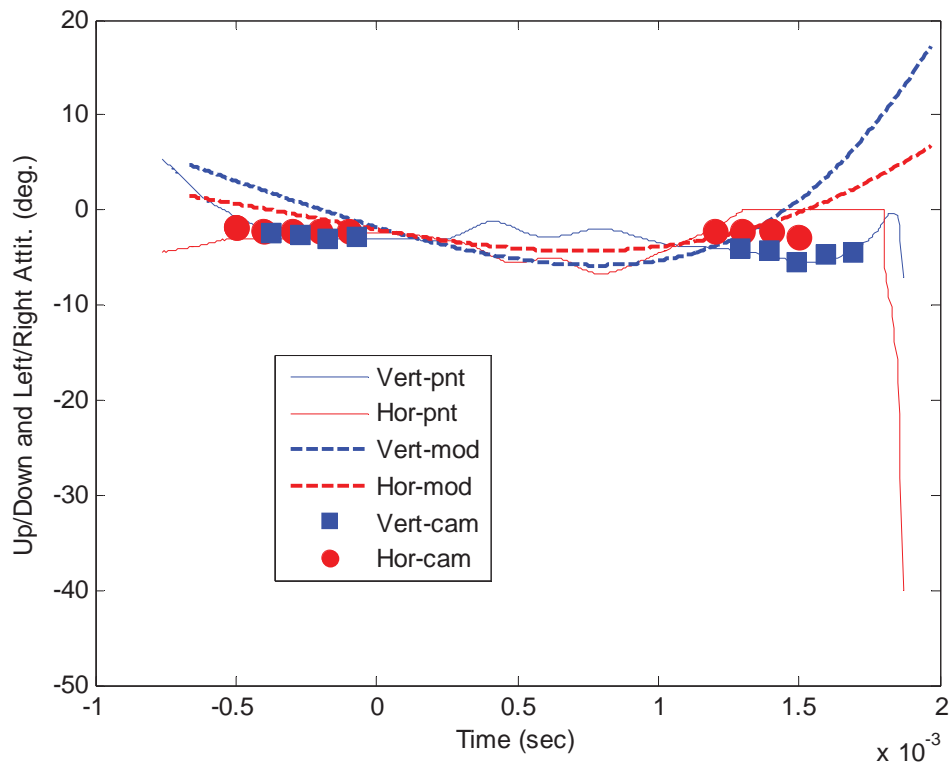
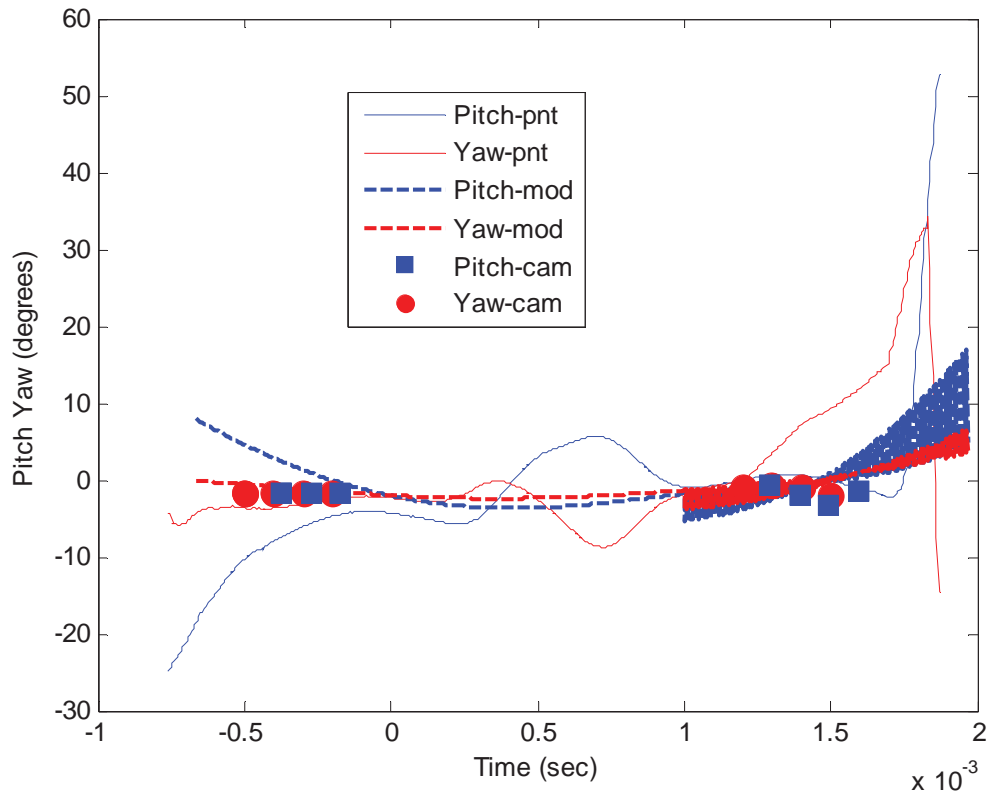


Figure 36. Up/Down and Left/Right Attitude Estimations with “*fminsearch*” (pt-pt), Polynomial Model (model) and Camera (cam) (Positive is up and to the right)



**Figure 37. Pitch and Yaw Estimations with “*fminsearch*” (pt-pt), Polynomial Model (model) and Camera (cam)**

## 7.0 CONCLUSION

In this study, two new tracking approaches were proposed, and the performance of the Matlab’s curve fitting and optimization algorithms were evaluated. In addition, 4 different sensor configurations were considered and their performances were compared.

The developed magnetic sensor method at the Munitions Directorate, AWEF, was found very promising. The experimental setup was very well planned and data were very clean. Tracking 6 variables, continuously is a very challenging task.

One of the tracking approaches calculated the B-field by integrating the measured coil voltages and estimated 6 parameters. This approach was found more reliable. The second approach estimated the location, orientation and their rates. The number of estimated parameters and number of equations were doubled. The voltage readings of two consecutive samplings were used for estimation of 12 parameters. The estimations were very good when the motion was smooth; however, the first method was more reliable when the projectile changed the direction quickly.

Four different sensor configurations were evaluated. Eight sensors located at the corners of the observation space were found the best approach based on convenience and accuracy. The

estimation accuracy was the best when ten sensors were used. The six sensor configuration also worked well; however, eight sensor configurations was slightly better. The results suggested using only the data of some sensors according to the location of the projectile when twelve sensors are used.

Nelder-Mead algorithm “*fminsearch*” + nonlinear curve fitting “*nlinfit*” combination was found as the best approach for implementation of the proposed tracking method. “*fminsearch*” estimated the initial values of the parameters. The “*nlinfit*” improved these estimations. Since, the “*nlinfit*” did not improve the estimations in some cases; the proposed algorithm evaluated the sum of the squares of both algorithms and used the estimations of the one which has the lower sum of the squares. This algorithm worked very well on the simulated data and a very complex motion of a magnetic projectile was followed with the average absolute positional error was better than 0.08 millimeter. Addition of noise to the simulated coil data reduced the accuracy of the estimations.

The performance of the selected tracking approach which estimated six parameters after integrating the voltage readings to obtain the B-field values was evaluated on the experimental data. The results of the polynomial model, proposed approach and results of the analysis of the images of the high speed cameras agreed for most of the experimental cases.

## 8.0 FUTURE WORK

The experimental configuration discussed in this paper is convenient for the experimental conditions where the impactor does not stray from the shot line and does not rotate. In theory, it is possible to extend this approach to include multi-axis motion and impactor rotation. The same optimization approach would apply, but the gauge models would be much more complicated and ought to be derived from simulations which accurately predict the magnetic flux as a function of position, motion, and rotation. Such simulations were performed in preparation for the current work. Based upon these simulations it was decided to initially implement a single-axis system without rotation. Among the lessons learned from these simulations are that the gauge size is very important. Smaller gauges are less sensitive because they integrate the changes in magnetic flux over smaller volumes. On the other hand, the gauge models are simpler for smaller gauges. Based upon these findings it is speculated that a multi-axis system might benefit by changing from induction coil gauges to other small, rapid-response magnetic field strength gauges. However, this approach has tradeoffs as well. At least 5 gauges would have to observe the impactor at any point to estimate X, Y, Z position and pitch and yaw. Thus, the total number of gauges would be large. Also, the other gauges may or may not be dependent upon the impactor velocity. If so, the gauge model becomes much more complicated as the velocity dependence must be incorporated as a function of the velocity vector orientation relative to the gauge. Perhaps more importantly, the velocity dependence is critical to the ability to estimate the impactor state – including both position and velocity – and allow only a single differentiation to obtain impactor acceleration.

## 9.0 ACKNOWLEDGEMENTS

The work was supported by the Summer Faculty Fellowship Program (SFFP) of the American Society of Engineers in Education (ASEE). The author thanks to the Munitions Directorate of the Air Force Research Laboratory for giving this opportunity to work at the Eglin AFB, FL.

### REFERENCES

1. Brian D. Reding, "Development of Particulate Materials Meso-Scale Diagnostic (PMMD) System, Final Report for SFFP Program, Summer 2012 report.
2. M. A. Ambroso, R. D. Kamien and D. J. Durian, "Dynamics of shallow impact cratering," *Physical Review*, 2005.
3. J. S. Uehara, M. A. Ambroso, R. P. Ojha and D. J. Durian, "Low-Speed Impact Craters in Loose Granular Media," *Physical Review Letters*, 2003.
4. M. Hou, Z. Peng, R. Liu, Y. Wu, Y. Tian, K. Lu and C. K. Chan, "Projectile impact and penetration in loose granular bed," *Science and Technology of Advanced Materials*, 2005.
5. H. Katsuragi and D. J. Durian, "Unified force law for granular impact cratering," *Nature.com*, 2007.
6. B. J. Jensen, D. B. Holtkamp, P. A. Rigg and D. H. Dolan, "Accuracy limits and window corrections for photon Doppler velocimetry," *Journal of Applied Physics*, 2007.
7. D. T. Berry, S. J. Bless, C. Waller-Delarosa and W. Lawhorn, "Ballistic Penetration of Sand: Preliminary," in *59th Meeting of the Aeroballistic Range Association (ARA)*, Cape Town, 2008.
8. W. A. Allen, E. B. Mayfield and H. L. Morrison, "Dynamics of a Projectile Penetrating Sand," *Journal of Applied Physics*, 1956.
9. W. L. Cooper and B. A. Breaux, "Grain fracture in rapid particulate media deformation and a particulate media research roadmap from the PMEE," *Springer Science & Business Media*, 2010.
10. R. L. Sierakowski, L. E. Malvern, J. A. Collins, J. E. Milton and C. A. Ross, "Penetrator Impact Studies of Soil/Concrete," *US Air Force Office of Scientific Research*, 1977.
11. D. W. Baum, R. M. Kuklo, J. E. Reaugh and S. C. Simonson, "Time-Resolved Diagnostics for Concrete Target Response," *International Journal of Impact Engineering*, pp. 93-100, 1997.
12. J. R. Royer, E. I. Corwin, P. J. Eng and H. M. Jaeger, "Gas-Mediated Impact Dynamics in Fine-Grained Granular Materials," *Consortium for Advanced Radiation Sources*, 2007.
13. J. A. Collins and R. L. Sierakowski, "Studies on the Penetration Mechanics of Eglin Sand," *Air Force Armament Laboratory*, 1976.
14. R. L. Moody and C. H. Konrad, "Magnetic Induction System for Two-Stage Gun Projectile Velocity Measurements," *Sandia Report*, 1984.
15. I.N. Tansel, B. Reding, W. L. Cooper, "Lagrangian Point State Estimation with Optimized, Redundant Induction Coil Gages," *Experimental Mechanics*, Published online: 17 January 2013, DOI 10.1007/s11340-013-9714-9.
16. J. A. Nelder and R. Mead, "A simplex method for function minimization," *Computer Journal* 7 (1965), 308-313.
17. Lagarias, J.C., J. A. Reeds, M. H. Wright, and P. E. Wright, "Convergence Properties of the Nelder-Mead Simplex Method in Low Dimensions," *SIAM Journal of Optimization*, 9.1(1998), 112-147

**DISTRIBUTION LIST**  
**AFRL-RW-EG-TR-2014-005**

Defense Technical Information Center      1 Electronic Copy (1 File & 1 Format)  
Attn: Acquisition (OCA)  
8725 John J. Kingman Road, Ste 0944  
Ft Belvoir, VA 22060-6218

---

EGLIN AFB OFFICES:

AFRL/RWOC (STINFO Office)	- 1 Hard (Color) Copy
AFRL/RW CA-N	- STINFO Officer Provides Notice of Publication
AFRL/RWMW	- 1 Copy